UNIVERSITÁ DEGLI STUDI DI NAPOLI

"FEDERICO II"

Dipartimento di Sanità Pubblica

Dottorato in

Sanità Pubblica e Medicina Preventiva

XXIX Ciclo

Coordinatore: Prof.ssa Stefania Montagnani

Tesi di dottorato di ricerca

PREPARATION AND ANALYSIS OF CUTANEOUS PRIMARY MYOFIBROBLAST THREE-DIMENSIONAL CULTURE: AN EXPERIMENTAL SYSTEM FOR MYOFIBROBLAST DEACTIVATION STUDIES

RELATORE: **CANDIDATO**

Prof.ssa Daria Anna Nurzynska **Dott.ssa Giuseppina Granato**

CO-RELATORE:

Prof. Alessandro Arcucci

CONTENTS

ABSTRACT **4**

Chapter 1 ..... **6**

INTRODUCTION **6**

1.1 Fibroblasts **6**

1.1.1 Origins, features and functions **6**

1.1.2 Fibroblasts differentiation into myofibroblasts **7**

1.1.3 Wound healing **11**

1.1.4 Cancer associated fibroblasts (CAFs) **12**

1.2 Three-dimensional cultures **13**

1.2.1 Three-dimensional versus two-dimensional culture **13**

1.2.2 Spheroids **14**

1.2.3 Techniques for the formation and growth of spheroids **15**

Chapter 2 ..... **19**

AIM OF WORK **19**

Chapter 3 ..... **21**

MATERIALS AND METHODS **21**

3.1 Cutaneous tissues **21**

3.2 Isolation of primary cutaneous fibroblasts and cell cultures **21**

3.3 Immunofluorescence analysis of fibroblasts **22**

3.4 Spheroid cultures **23**

3.4.1 Generation and growth **23**

3.4.2 Embedding, sectioning and deparaffinizing **24**

3.4.3 Histochemical and immunohistochemical staining **24**

3.4.4 TUNEL assay **24**

3.4.5 LDH assay **25**

3.4.6 Protein extraction and Western blotting analysis **25**

3.4.7 MTT assay **27**

3.4.8 Wound healing assay **27**

3.4.9 ELISA analysis **28**

3.5 Reversion of spheroids to adhesion and monolayer growth **28**

3.5.1 Preparation **28**

3.5.2 Cell cycle analysis **29**

3.5.3 Immunofluorescence analysis **29**

3.5.4 Protein extraction and Western blotting analysis **30**

3.6 Statistical analysis **30**

Chapter 4 ..... **31**

RESULTS **31**

4.1 Analysis of primary cells from skin of neck **31**

4.2 Fibroblast three-dimensional cultures **31**

4.2.1 Preparation **31**

4.2.2 Vimentin immunohistochemical analysis **32**

4.2.3 Evaluation of apoptotic cell death **32**

4.2.4 Evaluation of necrosis markers **33**

4.2.5 Evaluation of inflammation and activation markers **33**

4.2.6 Cell growth fraction evaluation **35**

4.3 Reversion of spheroids to adhesion and monolayer growth **35**

4.3.1 Evaluation of cell cycle phases **36**

4.3.2 Confocal immunofluorescence analysis **36**

4.3.3 Western blotting analysis **36**

4.4 Clusters and spheroids formed spontaneously **37**

Chapter 5 ..... **38**

DISCUSSION **38**

Chapter 6 ..... **44**

CONCLUSIONS **44**

Chapter 7 ..... **46**

ICONOGRAPHY **46**

Chapter 8 ..... **66**

BIBLIOGRAPHY **66**

ABSTRACT

Myofibroblasts are activated fibroblasts involved in tissue repair and cancer that are characterized by *de novo* expression of alpha smooth muscle actin (α-SMA), increased secretion of growth factors and immunoregolatory fenotype. It is known that myofibroblasts form clusters during cancer, fibrotic tissue and wound healing. At the end of wound healing, myofibroblasts undergo apoptotic cell death, whereas *in vitro* fibroblasts undergo a necrosis-like programmed cell death, called nemosis, associated with inflammatory response.

As primary myofibroblasts better resemble the tissue environment *in vivo,* in this work we generated spheroids from human primary cutaneous myofibroblasts to evaluate apoptotic or necrotic cell death, inflammation and activation markers during myofibroblasts clustering. The study showed that spheroid formation does not trigger apoptosis, necrotic cell death and cyclooxygenase-2 (COX-2) protein induction associated with inflammatory response. The significant decrease of α-SMA in protein extracts of spheroids, compared to myofibroblasts monolayer, led to hypothesize that myofibroblasts have undergone a deactivation process within spheroids. This hypothesis is supported by cytostatic effect exerted by spheroid-conditioned medium on both normal and cancer cell lines, by anti-migratory effect on normal cells and also by the low number of nuclei positive for the proliferation marker Ki-67. The analysis of spheroid reversion to monolayer growth demonstrated that fibroblasts cultured as aggregates preserved their proliferation capability. Surprisingly, we obtained spontaneous clusters by seeding myofibroblasts on plastic and glass substrates: thus the cluster formation could be a physiological feature of cutaneous myofibroblasts.

This work represents an experimental model to study myofibroblast deactivation and highlights the possible relevance of clusters as reservoir of myofibroblasts for regulating myofibroblast and tissue turnover.

Chapter 1

INTRODUCTION

1.1 Fibroblasts

1.1.1 Origins, features and functions

Human fibroblasts of the adult body represent a heterogeneous population of mesenchymal cells, with fusiform and spindle-shaped morphology with several cellular processes [1, 2, 3]. They are non-vascular and non-epithelial cells of the connective tissue, and are its principal cellular component. Furthermore, fibroblasts are not a homogeneous population even within a single tissue and are extremely versatile connective tissue cells [4]. In fact, it is known that connective tissue contains a mixture of distinct fibroblast lineages, with mature fibroblasts existing side by side with immature fibroblasts, often called mesenchymal fibroblasts, that have a remarkable capacity to differentiate into other members of the connective tissue family, including cartilage, bone, adipocyte and smooth muscle cells [5]. Fibroblasts of each part of the body can present different embryonic origins [3]: in fact, according to many authors, head and neck cutaneous fibroblasts are generated from the neural crest, hence derive from ectoderm, while cutaneous fibroblasts in most of other body regions are considered mesodermal cells [6, 7]. Fibroblasts from different sites also show different properties in proliferation, collagen synthesis as well as matrix metalloproteinase (MMP) expression under basal or inflammatory conditions, in migration and immunomodulatory function [89]. These features are maintained by fibroblasts *in vitro,* even after prolonged culture, reflecting their specific identity and positional memory [10]. In particular, fibroblasts isolated from different sites reflect a substantial topographic diversity and display distinct

and characteristic transcriptional patterns, suggesting that fibroblasts at different locations in the body should be considered distinct differentiated cell types [11, 12].

Fibroblasts can be easily isolated from tissues and cultured *in vitro*. They can be identified based on their fusiform morphology and expression of the fibroblasts specific protein-1 (FSP-1), desmin and vimentin, even if these markers are not specific of fibroblasts [3, 13]. The important functions of fibroblasts include the production, maintenance and renovation of the extracellular matrix (ECM) [13]. Indeed, fibroblasts synthesize many of the constituents of ECM, such as collagen type I, III and V and fibronectin, maintain ECM homeostasis by regulating ECM turnover and represent an important source of ECM degrading proteases such as MMPs. Apart from their function in healthy organs, fibroblasts also have a prominent role in remodelling and tissue repair and their activation is associated with immune responses [11]. In fact, fibroblasts can also acquire an immunoregulatory and activated phenotype triggering and upholding inflammation [2, 14]. In particular, fibroblasts modify the quantity, quality, and duration of the inflammatory infiltrate and play a critical role in the switch of acute resolving to chronic persistent inflammation [15].

1.1.2 Fibroblast differentiation into myofibroblasts

Differentiation of fibroblasts into myofibroblasts, i.e. fibroblast activation, is a complex process associated with distinct steps (*Figure 1*). In healthy tissue fibroblasts are maintained in an inactive state. During wound healing and in pathological conditions, such as inflammation and cancer, they become activated and differentiate into myofibroblasts that are morphologically and functionally different from fibroblasts [16]. Therefore, in intact and normal tissue, fibroblasts, stress-shielded by the crosslinked ECM, contain actin microfilaments into their cortical meshwork and they neither exhibit stress fibers nor form adhesion complexes with the extracellular matrix [17, 18], while

under mechanical stress, fibroblasts differentiate into proto-myofibroblasts which form stress fibers containing β- and γ-cytoplasmic actins [19]. Moreover stress fibers stretch between cells via *de novo* established N-cadherins type adherens juntions and to fibronexus adhesion complexes. The fibronexus is a specialized adhesion complex that uses transmembrane integrins to link intracellular actin with extracellular fibronectin fibrils [17]. Furthermore, proto-myofibroblasts express and organize cellular fibronectin, including the ED-A splice variant at the cell surface.

These features resemble those of fibroblasts that are isolated from various connective tissues or organs and placed onto plastic tissue culture dishes, in the presence of foetal calf serum [17]. Thereby, fibroblasts *in vitro* are mechanically activated, acquiring a proto-myofibroblast phenotype with stress fibers, focal adhesion and extracellular fibronectin fibrils [17, 19]. In particular, fibroblasts produce fibronectin messenger RNA, but these transcripts lack the two splice segments ED-A and ED-B [20]. However, during wound healing, these segments are included in the fibronectin mRNA and lead to *de novo* expression of ED-A fibronectin in the granulation tissue. Fibroblasts produce an ECM that contains cellular fibronectin including the ED-A splice variant also on rigid planar substrates [21].

Proto-myofibroblasts are always present where there is the need to generate mechanical tension and to proceed toward differentiated myofibroblasts, the main producers and organizers of extracellular matrix able to restore tissue integrity after injury. Myofibroblasts are characterized by *de novo* expression of alpha-smooth muscle actin (α-SMA), their most commonly used molecular marker [22, 23]. In culture, the presence of α-SMA in stress fibers confers to the differentiated myofibroblasts at least a twofold stronger contractile activity compared with proto-myofibroblasts. Furthermore, myofibroblasts are characterized by the presence of a contractile apparatus containing bundles of actin

microfilaments associated with contractile proteins, such as non-muscle myosin, and terminating at the myofibroblast surface in the fibronexus [23, 24]. Another characteristic of myofibroblasts is that, similarly to smooth muscle cells, they are connected directly to each other by specific cell-cell contacts, including adherens and gap junctions [18, 25]. The presence of intercellular junctions indicates that myofibroblasts could form multicellular contractile units within granulation tissue. In particular, gap junctions are composed of plasma membrane hemichannels that contain distinct and functionally related proteins called connexins. The connexin most expressed in myofibroblasts is connexin 43 [17, 26]. Different stimuli are responsible for the fibroblasts activation, including epidermal growth factor (EGF), platelet-derived growth factor (PDGF) and fibroblast growth factor-2 (FGF2), which are released from injured epithelial cells and infiltrating mononuclear cells, such as monocytes and macrophages [27, 28]. It is known that trasforming growth factor β1 (TGF-β1) has a key role in stimulating myofibroblast differentiation associated with collagen synthesis by fibroblastic cells [29, 30] and the expression of cellular fibronectin, particularly the ED-A splice variant [31]. Additionaly, fibroblasts are activated by direct cell-cell communication and contacts with leukocytes through adhesion molecules, such as intercellular-adhesion molecule-1 (ICAM-1) or vascular-cell adhesion molecule-1 (VCAM-1) [27], and by reactive oxigen species, or complement factor C1, as well as by the altered ECM composition [28]. It is also known that desmoplasia, i.e. disproportionate formation of the fibrous connective tissue, generates mechanical forces that convert fibroblasts to myofibroblasts and induces cancer cell growth, invasion, and metastasis. [14, 32].

Fibroblasts activation is associated with production of large amounts of cyclooxygenase-2 (COX-2) and proinflammatory cytokines, although the extent of fibroblast activation depends on the tissue type [2, 6]. The fibroblast activated phenotype, either in wound

healing, fibrotic or cancer tissue, is associated with *de novo* expression of α-SMA, increased levels of growth factor secretion and ECM-degrading proteases: this process is regulated by inflammation and represents the differentiation of fibroblasts into myofibroblasts [33, 34, 35]. Fibroblasts *in vivo* form clusters in cancer, fibrotic tissue and wound healing process [36]. Hovewer, *in vivo*, at the end of wound healing, activated fibroblasts undergo apoptotic cell death [37] *(Figure 2)*. On the contrary, fibroblasts *in vitro* undergo a necrosis-like programmed cell death, called nemosis, associated with inflammatory response [2, 38]. In particular, it is known that fibroblasts established from neonatal foreskin, when forced to cluster, do not grow but undergo a new pathway of cell activation, leading to a massive proinflammatory, proteolytic and growth factor response. The activation begins with fibronectin-β1, α5 and αV integrin interaction, in particular between the RGD motif of fibronectin and cellular integrin receptors [39], and terminates in programmed necrosis-like cell death. Previous studies carried out *in vitro* also showed that clusters of fibroblasts established from neonatal foreskin, named spheroids, are activated to produce massive amounts of COX-2, prostaglandins, proinflammatory cytokines and growth factors: this process is associated with nemosis, leading to spheroids decomposition [38]. Indeed, during nemosis, COX-2 protein is present accross the whole spheroid and not only in the centre where nutrient deprivation and hypoxia are presumably the highest, demostring that COX-2 induction is not triggered by hypoxia [2]. Moreover, it is well known that nemotic fibroblast spheroids stop their growth abruptly and after about two days begin to decompose, releasing massive amounts of lactate dehydrogenase (LDH), proinflammatory cytochines (IL-1, IL-6), chemokines (RANTES, IL-8), and growth factors such as hepatocyte growth factor/scatter factor (HGF/SF), involved in the promotion of cellular growth and motility. Additionally, it is also known

that fibroblasts clustered in spheroids are committed early to nemosis [38]. Interestingly, a recent work showed that nemosis is a reversible process [16].

1.1.3 Wound healing

Wound healing represents a physiological response to injury, ensuring rapid repair of damaged tissues, associated with fibroblast activation (*Figure 2*). It is a highly regulated process of consecutive and overlapping phases: immediately after tissue injury, the blood coagulation cascade induces inflammatory cell accumulation and cytokine production and the release of various growth factors [40]. Disruption of blood vessels also leads to the formation of the blood clot, which is composed of cross-linked fibrin, and of extracellular matrix proteins. Apart from providing a barrier against invading microorganisms, the blood clot also serves as a matrix for invading cells. Inflammatory cells invade the wound tissue and produce proteinases and growth factors that stimulate collagen production and initiate the proliferative phase of wound repair. At the wound edge, migration and proliferation of keratinocytes support re-epithelialization that involves the replication and movement of epidermal cell to reconstituite tissue continuity [40]. It is followed by proliferation of dermal fibroblasts in the neighborhood of the wound. These cells subsequently migrate into the provisional matrix and deposit large amounts of extracellular matrix. Furthermore, wound fibroblasts acquire a contractile phenotype and transform into myofibroblasts, a cell type which plays a major role in wound contraction. In this proliferative phase, in the wound bed a new tissue is formed, called granulation tissue because of the granular appearance of the numerous capillaries led by massive angiogenesis [41]. Together, these processes restore tissue integrity and reduce the wound size to a permanent scar [17]. In the final maturation phase, the overall numbers of fibroblastic cells and vessels are reduced by programmed cell death [42]. It is evident that

disturbance of the fine equilibrium between cells, growth factors, and ECM in any of these phases will impact on the normal course of healing [40].

In many instances, due to mechanisms not yet understood, scarring does not occur even despite epithelialization, and granulation tissue evolves into a hypertrophic-scar [43]. Wound healing and cancer progression have striking similarities [45]. Tumors have been described as "never-healing wounds" [44]. The mechanisms that regulate wound healing have been shown to promote transformation and growth of malignant cells [46]. Recently, inflammatory processes that occur during normal wound healing have been linked to the pathological state of many tumors. Motility is needed for the dissemination from the site of primary tumor leading to invasive phenotype [47]. Hence, wound healing studies appear useful for evaluating the migratory capability of both normal and cancer cells.

1.1.4 Cancer associated fibroblasts (CAFs)

Activated fibroblasts are also found in association with cancer cells, in fact they are known as cancer-associated fibroblasts (CAFs) *(Figure 3)*. CAFs, acting in a paracrine manner, are important promoters of invasion, tumour growth and progression [48, 49], as well as angiogenesis and metastatic process [13, 50, 51]. CAFs represent the most prominent cell type within the reactive stroma of many cancers, such as breast, prostate and pancreatic carcinoma [52]. In breast cancer, over 80% of CAFs are myofibroblast which are phenotipically and epigenetically different than normal dermal fibroblasts. Indeed, CAFs are considered a cell population in a permanently activated state, sharing similarities with fibroblasts activated during wound healing process [53]. Unlike them, CAFs neither revert to a normal phenotype nor undergo apoptosis [14] but, once the activating stimulus is attenuated, their presence persists in tumor stroma [17, 54]. The irreversible activation of CAFs is due to signaling pathways driven by several factors produced mainly by tumor cells and autocrine loops [14]. Several works indicate that

CAF activation is a redox-dependent process [14, 55]. Indeed, cancer tissues usually contain higher levels of reactive oxygen species (ROS) than normal tissues. Furthermore, it is known that ROS can be transferred from cancer cells to fibroblasts. In particular, ROS promote conversion of fibroblasts into highly migrating myofibroblasts through accumulation of the hypoxia-inducible factor (HIF-1α) trascription factor and the CXCL-12 chemokine [56]. CAFs can originate from resident stromal fibroblasts, bone marrow-derived fibrocytes or by epithelial/endothelial to mesenchymal transition [52]. Various markers are used to detect CAFs in cancer tissue and among these α-SMA is the most widely used [54].

1.2 Three-dimensional cultures

1.2.1 Three-dimensional versus two-dimensional culture

Traditional two-dimensional (2D) monolayer culture represents a simplified, reproducible and largely available system. Despite these features, it is recognized that plastic or glass substrates, commonly used for cell culture, are not representative of the cellular environment found in living tissue, due to the absence of the stroma that sustains the cellular architecture [57]. Cells grown in 2D monolayer culture lose tissue specific properties [58, 59] and thus do not reproduce the structural organization or functional differentiation of tissues *in vivo* [60]. Accordingly, moving from cell monolayers to three-dimensional (3D) cultures is motivated by the need to work with models that mimic the functions of living tissues. The third dimension bridges the gap between cell culture and tissue.

3D cell cultures have been widely used in biomedical research since the early decades of this century. They are able to investigate aspects of tumor biology and pathophysiology, by maintaining a 3D cancer cell arrangement that reflects the *in vivo* normal and cancer tissue situation in relation to cell-cell and cell-ECM interactions and differentiation

patterns [61]. Furthermore, 3D cell cultures can be used to study the interactions between stromal cells, such as fibroblast, and cancer cells [36]. Therefore, 3D cultures could better reflect the *in vivo* behavior of cells in tumor tissues [62]. One major advantage of 3D cell cultures is their well defined geometry, which allows to directly relate structure to function of 3D cell cultures and enables theoretical analysis, including diffusion fields. [63]. 3D cultures are currently used in a broad range of cell biology studies and biomedical research [64], including tumour biology [65], cell adhesion, cell migration and epithelial morphogenesis, as well as drug screening [66, 67].

1.2.2 Spheroids

The most widely used 3D tissue culture model involves cellular aggregates, called spheroids, where cells have a spherical, organised and compact symmetry [57], which have been proposed by radiobiologists in 1970. Initially, tumor spheroid cultures were applied in experimental radiotherapy, followed by photodynamic treatment, hyperthermia and chemotherapy and in preclinical drug evaluation [68, 69, 70]. Cellular spheroids are simple 3D systems, which take advantage of the natural tendency of many cell types to aggregate [57]. They can be obtained from single cultures or co-cultures, as mono or multicellular spheroids (MCS), respectively.

Multicellular tumor spheroids (MTS) present many of the characteristics of *in vivo* tumors, which are unavailable in monolayer cells, and as such, they have gained increasing recognition in biomedical research [71]. MTSs are able to accurately mimic some features of solid tumors, such as their spatial architecture, physiological responses, secretion of soluble mediators, cell morphology, growth kinetics, gene expression patterns, tumor cell invasion and metastasis [63]. Currently, several works describe MTS as a tumor model in drug and radiotherapy research. Besides sharing many biological

similarities with avascular tumors, MTSs also display elevated resistence to chemo- and radio-therapies and produce biochemical response mimicking parental tumors. These properties make MTS more predictive of the *in vivo* therapeutic efficacy [68, 72] and drug resistance mechanisms [73, 74]. In addition, MCSs hold great promise to be used as building blocks in organ printing for the construction of hybrid artificial organs [75].

Spheroids can be a useful tool to study the tissue turnover regulated by fibroblasts. In fact, it is known that activated fibroblasts form clusters in wound healing process, idiopathic pulmonary fibrosis and hypertrophic scars, where cells clusters are formed by nodules of myofibroblasts [36, 43]. A recent work detected fibroblast aggregates in the dermis at early stages of melanoma development, before metastasis formation, and showed a paracrine communication between cancer cells and fibroblasts [76]. However, the growth of fibroblasts as spheroids can be associated with conditions where fibroblasts lose their contact to connective tissue. Additionaly, fibroblasts can lose their contacts to ECM during inflammation, wound healing and cancer [16].

1.2.3 Techniques for the formation and growth of spheroids

Up to now, a variety of techniques have been developed for the formation and growth of multicellular spheroids [64], in order to obtain cellular aggregation encouraging cell-cell contacts and avoiding traditional cell-plastic substrates. A simple and reproducible method for generating spheroids is a prerequisite for spheroid-based applications. Among the known strategies, the oldest is the "spinner flask" method [77], where cells are maintained in spinner flasks and the constant movement prevents their attachment to the walls of the flask and allows them to attach to each other and grow as aggregates [78] *(Figure 4A)*. Comparable methods use roller tubes, gyratory shakers or rotating wall vessels [79] which keep the cell suspension in continuous agitation between

rotating cylindrical walls [80] (*Figure 4B*). Using these culture vessels for spheroids production, the spheroid can suffer from a rather strong shear force, which may affect cell physiology. To overcome this problem, an improved rotary cell culture system has been designed to create a unique microgravity environment with low shear force [80]. These methods are suitable for large scale production. However, they have not been used by a lot of researches due to their drawbacks, including the generation of numerous heterogeneously sized spheroids, the inability to study individual spheroid for prolonged periods, the need for large volume of media culture and specialized equipment.

Other techniques are based on the loss of an appropriate surface for cell attachment that might promote MCS formation, just as the constant agitation does in the spinner flask system (*Figure 4C*). The growth of spheroids is feasible over plates made of nonadhesive plastics or plates made nonadhesive for cells by coating with a thin nonadherent film. Agarose represents one of the most efficient substrates to prevent cell attachment [67, 81], followed by hydrophobic polymers, including nonionic compound poly2-hydroxyethymethacrylate (polyHEMA) [82], which also prevents matrix deposition and subsequent cells attachment. The use of nonadherent surfaces for cells frequently yields delicate numerous aggregates with highly irregular geometry. Consequently, obtaining aggregates of roughly equal size and shape requires manual selection and/or screening [72]. Furthermore, effects on the cells due to physical forces or chemicals can not be excluded [83]. These methods have also the drawbacks of being tedious, manually intensive and with a limited scope for mass production.

To address many of the problems identified above, tissue engeenering has developed a more advanced 3D cancer models using biological gels as a substrate for spheroid growth. The earliest attempts to grow cancer cells within 3D substrates use small explants of cancer tissue within a natural gel. Because of its ubiquitous nature and relative ease of isolation,

collagen is one of the earliest biomaterials to be widely used for 3D cell culture [84]. This method is used to culture a wide variety of cancer types in a way that preserves the native tissue architecture and cell viability. Other natural polymer gels that have been used are the alginate, a natural polymer derived from brown seaweed that gels in the presence of calcium ions, and the Matrigel, a basement membrane extract derived from the Engelbreth-Holm-Swarm mouse sarcoma [67, 70].

Spheroids are also produced by the "hanging-drop" method [85, 86] which was first applied to the embryonic stem cells that are able to differentiate forming embryoid bodies [87, 88] (*Figure 4D*). In this method, cells are suspended in droplets of medium, diluted to the desired cell density, and dispensed onto the lid of a tissue culture dish. When the lid is inverted, each drop is held in place by surface tension and cells accumulate at the free liquid-air interface falling to the bottom of the drop. This natural disposition of cells pushes them to aggregate. Such approach represents an attractive alternative for MCS production, because it is simple, highly reproducible, can be applied successfully to a wide variety of cell lines and can produce spheroids in short time and of a homogeneous size without the need for sieving or manual selection. However, there are several disadvantages of the hanging-drop method: the liquid volume of a drop is limited to less than 30 μl, a direct microscopic observation of forming drops is difficult during cultivation and, in particular, the inability to change the medium culture make the technique suitable only for short-term experiments [89]. For a lot of applications it is important that generated spheroids are uniform in shape and size [75, 90]. In order to control spheroids size and geometry and to have their massive production, many authors used microstructures to guide the multicellular self-assembly; the most widely exploited are "microwells" [91] (*Figure 4E*). Microwells of defined size and different geometry can be fabricated by microfabrication techniques such as micromolding of cell-nonadhesive

inert materials like agarose or polyethylene glycol (PEG) [92, 93]. Suspended cells are loaded onto the fabricated device, redistribuited by gravity and hydrodynamic forces, and eventually assembled into aggregates according to microwell geometry. This method has some limits, as the complicated fabrication of the microstructures requires specialized facilities and the use of a template and specific cell culture plates.

Recently, Zhao *et al*. showed that the poly (2-hydroxyethyl methacrylate) PHEMA hydrogel film with swelling-induced wrinkling surface pattern can be used for MCS generation [94] (*Figure 4F*). Unlike previously reported studies, the patterned hydrogel films were generated spontaneously without the use of any template or specialized facilities, directly in the wells of commercial cell culture plates and were able to guide the self-assembly of cells. Swelling of the film in water produces various wrinkling patterns composed of uniformed microcaves on the film surfaces. When cell suspension is added, the cells settle down by gravity to the bottom, accumulate to the center of the microcaves and gradually self-assemble into MCSs. Thousands of the spheroids can be generated in a single well, with uniform size that can be controlled by the number of cells seeded. Despite the existence of various tecniques that can potentially facilitate MCS formation, there is currently no standard method to apply for every use. Hence, the research and the choice of the suitable method depend on the cell type used and on the scope of the study. Often, the available methods need to be combined for obtaining the MCS with the required characteristics. Fortunately, MCS-based 3D culture models continue to advance in all aspects, including methodology in generation and manipulation of spheroids in order to totally satisfy all needs.

Chapter 2

AIM OF WORK

The activation of fibroblasts is represented by their differentiation into myofibroblasts, a process characterized by the expression of α-SMA, increased levels of growth factors and ECM-degrading proteases. Clusters of activated fibroblasts have been observed in physiological and pathological conditions such as wound healing process, idiopathic pulmonary fibrosis, hypertrophic scars and cancer [36, 43]. In particular, a recent study detected fibroblast aggregates in the dermis at the early stages of melanoma development, before metastasis formation, and showed a paracrine communication between cancer cells and fibroblasts [76]. The turnover of activated fibroblasts is *in vivo* associated with apoptotic cell death, whereas *in vitro*, fibroblasts undergo a necrosis-like programmed cell death, called nemosis, associated with inflammatory response [37].

The aim of the work was to produce and analyze clusters, called spheroids, of human primary myofibroblasts from normal skin of neck. Primary myofibroblasts have been chosen for the generation of spheroids, as they should better recall the *in vivo* tissue properties, as opposed to the estabilished cell lines used by several other research groups. The first goal of the evaluation was to determine the type of cell death, apoptotic or nemotic, in order to understand how the activated fibroblasts are regulated following spheroids formation; further analyses included the evalutation of the inflammation and activation markers, in order to define whether the myofibroblasts within spheroids *in vitro* are quiescent or activated.

Myofibroblast are involved in the response to injury in physiologial and pathological conditions. As such, they have a prominent role in the progression, growth and spread of

tumours. Given these premises, it has been considered important to analyze also the paracrine interaction between spheroids and both normal and cancer cells. Finally, we evaluated the possibility of reversion of spheroids to monolayer growth *in vitro*.

By providing the answers to the above questions and determining the features of the myofibroblasts *in vitro*, the present study should further our knowledge on fibroblast contribution to the organ architecture in physiological and pathological conditions In particular, it could represent an experimental system to study fibroblast activation/deactivation process, with a possible application in modulation of unwanted tumor progression and massive myofibroblast persistence in connective tissue diseases.

Chapter 3

MATERIALS AND METHODS

3.1 Cutaneous tissues

Normal human skin specimens were obtained from donors (n:7 females, mean age 48 ± 2.5 years) undergoing neck surgery for benign pathologies. Patients with metabolic and connective tissue diseases were excluded. The investigation was in agreement with the principles outlined in the Declaration of Helsinki [95] and informed consent from all patients was obtained.

3.2 Isolation of primary cutaneous fibroblasts and cell cultures

Human cutaneous fibroblasts were obtained by using an explant technique. The surgical tissue was minced into small fragments (< 1mm) that were washed, placed into 35-mm Petri dishes (BD Falcon, Bedford, Massachusetts, USA) and covered with covering glasses and grown in Dulbecco's minimal essential medium (DMEM) (Sigma-Aldrich, Saint Louis, Missouri, USA), supplemented with 10% fetal bovine serum (FBS) (GIBCO, Grand Island, New York, USA), 200mM L-glutamine, antibiotics (100 mg/ml penicillin, 100 mg/ml streptomycin) (all purchased by Sigma-Aldrich). The plates were maintained at 37°C with 5% CO_2 and 95% humidity in a HeraCel (Heracus) incubator, with fresh culture medium changed every 3 days. The time required for fibroblast cells outgrowth from bioptic fragments was highly variable, usually it took around two weeks. At 75% cell confluence, fragments were removed while cells were detached by mild trypsinization with 0.25% trypsin-EDTA (Sigma-Aldrich) for 5 min at 37°C, and

replated, thereby promoting fibroblasts isolation. All experiments were performed using cells only from early passage, within the eighth passages.

The human keratynocyte (HaCat) and fibrosarcoma (HT1080) cell lines were kindly provided by CEINGE (Naples, Italy). Both cell lines were cultured in DMEM under the same conditions, as described above. Cells were observed with a phase contrast microscope Olympus CKX41 model and the images were acquired with a camera connected to its by means Cell-A software.

3.3 Immunofluorescence analysis of fibroblasts

Morphological analysis of fibroblasts was performed by plating 5 x 10^4 cells on glass coverslips (Bio-Optica, Milan, Italy). Once adherent cells were more than 75% confluent, they were washed in 1X PBS, fixed in 4% paraformaldehyde (Merk Millipore, Billerica, Massachusetts, USA) for 20 minutes at room temperature and at least washed again, according to standard techniques. Then cells were permeabilized with 0.1% Triton X-100 (VWR International Srl, Milan, Italy) and blocked in donkey serum (Merk Millipore) diluited 1:10 in 1X PBS, for 30 min at room temperature. Glass coverslips (Bio-Optica) were incubated for 1 hour at 37°C, with primary antibody against mouse monoclonal vimentin (Sigma Aldrich) diluited 1:80. After three washes in PBS, the cells were incubated with fluorescein-conjugated donkey anti-mouse secondary antibody (Jackson ImmunoResearch Europe, Newmarket, UK) diluted 1:50. F-actin was stained with rhodamine phalloidin (Sigma-Aldrich) diluted 1:100 for 1 hour at 37°C. Nuclei were counterstained with DAPI (Merck Millipore). Glass coverslips were mounted in Vectashield (Vector Labs, Peterborough, UK). Microscopic analysis was performed with a Leica DMLB microscope equipped with epifluorescence EL6000 system (Leica Microsystems, Wetzlar, Germany). Pictures were taken with digital camera (Leica

DFC345FX) connected to the microscope and then merged with the software Leica Application Suite.

3.4 Spheroid cultures

3.4.1 Generation and growth

Human primary fibroblasts spheroids were produced adapting the previously described hanging-drops and coated plates methods [96]. Fibroblasts were detached from culture dishes by trypsin/EDTA (Sigma-Aldrich), harvested, diluted and 20µl of cell-suspension drops, containing 1 x 10^4 cells, were put on lids of 96-well plates (BD Falcon) and the tray was inverted. Moreover, into each of the wells were added 100 µl of 1X PBS to avoid culture medium evaporation. After 12h of incubation at 37°C, the drops were transferred to agar-coated U-bottom 96-well plates (BD Falcon), containing 80µl of DMEM. For agar coating, the U-bottom 96-well plates were pre-treated with 1% agarose (Applichem, Gatersleben, Saxony-Anhalt, Germany) dissolved in 1X PBS, autoclaved and dispensed into each well (100 µl/well) and let to solidify, in order to form a thin film of a nonadhesive surface. The formation of the fibroblast spheroids was observed at a phase contrast microscope and photographed at 24h, 48h, 72h and 96h after plating. The size of the single spheroids was estimated by measuring two orthogonal diameters (d1 and d2) using Cell-A software. Spheroid volume was determined according to the formula: $V=4/3\pi r^3$ where $r= 1/2 \sqrt{d1xd2}$ [96]. Mean diameters and mean volumes were calculated for each timepoint.

Spontaneous spheroids were obtained from 5 x 10^4 cells seeded onto the bottom of 12-well plastic plates (BD Falcon) or glass plates (MatTek corporation, Avenue-Ashland, Massachusetts, USA) and maintained in culture for several days.

3.4.2 Embedding, sectioning and deparaffinizing

Spheroids were collected at 24h, 48h, 72h and 96h, fixed in 10% neutral buffered formalin (Bio-Optica) and embedded in paraffin (Bio-Optica), according to the standard protocol. Serial 4μm-thick sections were obtained by a Leica Supernova ultramicrotome and placed on poly-L-lysine coated glass slides (Menzel-Glaser, Brunswick, Germany). Slides were deparaffinized twice in xylene and rehydrated in graded series of ethanol, and immersed in 10 mM citric acid (Sigma-Aldrich), pH 6, in a microwave oven (VWR) for three cycles of 5 minutes at 650 Watt, to exclude epitope masking owing to fixation. This procedure was performed before proceeding to every subsequent staining.

3.4.3 Histochemical and immunohistochemical staining

Spheroids deparaffinized sections were stained, for morphological analysis, with haematoxylin and eosin (Bio-Optica) according to the manufacturer's protocol. Other deparaffinized sections were immunostained with primary antibodies against mouse monoclonal vimentin or rabbit monoclonal Ki-67 (both Ventana Medical System, Tucson, Arizona, USA) detected by ULTRA View UNIVERSAL DAB DETECTION KIT (Ventana Medical Systems), diluted 1:100, according to the manufacturer's protocol. Glass coverslips were always mounted with BioMount (Bio-Optica). Microscopy analysis was performed with a Leica DMLB microscope. Images were captured in bright field with a digital camera Leica DC200 (Leica Microsystems) connected to the microscope.

3.4.4 TUNEL assay

A method for examining apoptosis via DNA fragmentation is by the terminal deoxynucleotidyl transferase (TdT)-mediated dUTP nick-end labeling (TUNEL) assay [97]. TUNEL staining was performed on spheroids sections, deparaffinized and rehydrated as described above, using ApopTag Plus Fluorescein In Situ Apoptosis Detection Kit (Merck

Millipore), in accordance with the manufacturer's protocol. In brief, sections were covered with terminal deoxynucleotidyl transferase working solution and incubated for 1 hour at 37°C in a humidified chamber. The reaction was stopped by incubation with stop/wash buffer. After three washes with PBS, antidigoxigenin fluorescein isothiocyanate was applied to the slides for 30 minutes at room temperature. Cell nuclei were counterstained with DAPI and the stained area of sections were washed in PBS and mounted under a glass coverslip in Vectashield (Vector Labs). Microscopic analysis was performed with a Leica DMLB microscope equipped with epifluorescence EL6000 system (Leica Microsystems). Pictures were taken with digital camera connected to the microscope (Leica DFC345FX) and then merged with the software Leica Application Suite. Number of nuclei was calculated using Image J software with Cell Counter plugin. The ratio of apoptotic cells was expressed as a percentage of positive cells among all cells in a spheroid at each timepoint.

3.4.5 LDH assay

The cytotoxicity and cell decomposition in the culture media were evaluated by lactate dehydrogenase (LDH) enzymatic activity assay. To this aim, cutaneous myofibroblasts seeded at 1 x 10^4 cells/well were grown as monolayer or spheroid cultures. At selected time points, the aliquots of cell-conditioned medium were added to 1ml of the reaction mixture containing 0.1M Tris-HCl, pH 7.5, and 125µM NADH. The reaction started with the addition of 600µM sodium pyruvate and was followed by the decrease in absorbance at 340 nm. The results were normalized to the LDH activity in 100% death caused by fibroblast freezing and thawing.

3.4.6 Protein extraction and Western blotting analysis

Total protein extracts were prepared from fibroblasts monolayer, harvested by tripsin/EDTA, and from fibroblasts spheroids collected at 24h, 48h, 72h and 96h.

Samples were incubated on ice-cold for 30 min in a RIPA lysis buffer containing 50mM Tris-HCl (pH 7.4), 150mM NaCl, 1% Nonidet P-40, 0.25% sodium deoxycholate, 1mM NaF and 1mM Na_3VO_4, supplemented with proteases inhibitors cocktails (1mM DTT, 2mM PMSF, 2μg/ml aprotinin and 10μg/ml leupeptin) (Roche Diagnostics Corporation, Mannheim, Germany). Lysates were centrifuged at 12000g for 30 min at 4°C and protein concentration in the supernatants was determined by the Bradford method (Bio-Rad Laboratories, Hercules, California, USA) [98]. Albumin from bovine serum (BSA, Sigma-Aldrich) was used to construct the standard curve. The absorbances were read by Cary Eclipse spectrophotometer (Varian, Santa Clara, California, USA) at 595 nm. Western blotting was performed with equal amounts of total protein extracts (20μg). Briefly, protein samples were dissolved in SDS-sample buffer and were size-fractionated by electrophoresis on 10% SDS-polyacrylamide gel, under reducing and denaturing conditions at 120V and transferred onto a polyvinylidene difluoride (PVDF) membrane (Merck Millipore) at 360mA for 90 minutes. Molecular weight marker was loaded onto gel as a weight indicator. The membranes were blocked and then incubated for 1 hour with one of the following antibodies: COX-2 (Sigma Aldrich), α-SMA (Abcam, Cambridge, UK), GAPDH for loading control (Cell Signaling Technology, Massachusetts, USA), all diluted 1:1000, followed by horseradish peroxidase-labelled specific secondary IgG antibodies (all from Santa Cruz Biotechnology, Santa Cruz, California, USA) 1:15000 for another 1 hour at room temperature. Antibody binding was analysed by an enhanced chemiluminescence reaction, using Super Signal West Femto Maximum Sensitivity Substrate Kit (Thermo Scientific, Rockford, Illinois, USA) according to the manufacturer's instructions and visualized by autoradiography (Kodak Company, Rochester, New York, USA). Images were acquired by Epson Perfection 2480 Photo (Epson, Suwa, Japan). The intensity of individual bands was determined using ImageJ software.

3.4.7 MTT assay

To evaluate the influence of the culture medium conditioned by the fibroblast primary spheroids and monolayer on the proliferation of the normal HaCat and cancer HT1080 cells, the 3-(4,5-dimethylthiazol-2-yl)-2,5-diphenyltetrazolium bromide (MTT) cell proliferation assay was used. The MTT is an indicator of cell viability and the assay was performed according to manufacturer's protocol. Conditioned medium was prepared by culturing cutaneous fibroblasts (1×10^4) in DMEM, grown as monolayer and spheroid cultures, and collected at 72h. HaCat and HT1080 cells were seeded on 96-well plates (1×10^4). After 24 hours, the culture medium was replaced with 100µl of conditioned medium from spheroid or monolayer cultures of fibroblasts. After 48h of incubation, 10µl of 12mM MTT reagent (5mg/ml, Sigma-Aldrich) was added to each well and incubated for 3 hours at 37°C in 5% CO_2 incubator. Then, culture medium was removed and 100µl of solubilization solution (0.01M HCl in isopropanol) was added to each well to dissolve the formazan crystals. Absorbances was measured at 540 nm using Multiscan EX microplate reader (Thermo Labsystems, Vantaa, Finland).

3.4.8 Wound healing assay

Spheroid- and monolayer-derived conditioned medium, both preparated as described above, was used to evaluate the migratory response of HaCat and HT1080 cells in the wound healing assay. It is a simple and reproducible method commonly used to assess cell motility into the wound space [99]. To this aim, $2{,}5 \times 10^5$ cells were seeded into 35mm tissue culture plates and were grown to confluence. Then, the confluent monolayer of cells was carefully scratched with a sterilized pipette tip. After wounding, the plates were rinsed twice with 1X PBS to remove cell debris. Cells were incubated with either spheroid- or monolayer-conditioned medium collected after 72 hours of culture. Photographs of the same fields were taken at 0h, 4h and 24h with a camera connected to a

phase contrast microscope Olympus CKX41 model and the images were acquired using Cell-A software. Quantitative analysis of open wound was performed by measuring the gap area at different timepoints using ImageJ Software (National Institute of Health, USA). The ratio between the relative open surface area at indicated timepoints and at baseline was calculated.

3.4.9 ELISA analysis

Identical aliquots of fibroblasts (1 x 10^4) were simultaneously cultured as monolayer and multicellular clusters, as previously described, and the conditioned medium was collected at 72h to evaluate the secretion of HGF by the cells *in vitro*. The concentration of HGF was estimated by Enzyme-linked immunosorbent assay (ELISA), using Human HGF kit (RayBiotech, Norcross, GA) in accordance with manufacturer's instructions. This assay employs an antibody specific for human HGF coated on a 96-well plates. Standards and samples were pipetted into the wells and HGF was bound to the wells by the immobilized antibody. The wells were washed and biotinylated anti-human HGF antibody was added. After washing away unbound biotinylated antibody, HRP-conjugated streptavidin was pipetted to the wells. The wells were again washed, a TMB substrate solution was added to the wells and color developed in proportion to the amount of bounded HGF. The Stop Solution changed the color from blue to yellow, and the absorbance at 450 nm was determined using a spectrophotometer Multiscan EX microplate reader (Thermo Labsystems). The concentration of HGF was calculated from the standard curves.

3.5 Reversion of spheroids to adhesion and monolayer growth

3.5.1 Preparation

Multicellular aggregates were photographed and then collected from agar-coated U-bottom 96-well plates after 96 h and 216 h of tridimensional culture and cultured in 60-mm

standard plastic dishes (BD Falcon) or on glass coverslips (Bio-Optica). In order to test the possible outgrowth of fibroblasts from spheroids and to evaluate the reversion of spheroids to adhesion and monolayer growth, spheroids were observed daily.

3.5.2 Cell cycle analysis

First, cell cycle of cells outgrown from spheroids cultured for 96 h and 216 h on agar and reverted to adhesion growth for twelve days were analyzed with the Cell-Clock Mammalian Cell Cycle Assay (Biocolor, North Irland, UK), performed according to the manufacturer's protocol. This assay is a live-cell detection employed to monitor the different phases of cell cycle during *in vitro* culture. It uses the one-hour incubation at 37°C with a redox dye that is taken up by live cells and undergoes a distinct color change. In particular, it is yellow in the reduced form, green in the intermediate state, and turns blue in the fully oxidised form; these color changes indicate cells in the G1, G2 and M phases, respectively.

Cells were observed at a Leica DMLB microscope (Leica Microsystems). Images were taken within 15 min from the end of staining procedure in bright field with a digital camera (Leica DC200; Leica Microsystems) connected to the microscope.

3.5.3 Immunofluorescence analysis

Spheroids cultured for 96 h and 216 h on agar as tridimensional culture and reverted to adhesion growth for twelve days were fixed with 4% paraformaldehyde (Merk Millipore), washed twice in 50mM NH_4Cl, and permeabilized as previously described [100] Double immunostaining was performed using a primary mouse vimentin antibody (Sigma-Aldrich) and rhodamine phalloidin, as described in paragraph 3.3. Nuclei were stained with DAPI. Immunofluorescence analysis was performed with a confocal laser scanning microscope LSM 700 (Zeiss, Gottingen, Germany). Fluorescence emission was revealed by 460-489

band pass filter for DAPI; 505-530 band pass filter for FITC, and by 560–615 band pass filter for TRITC. Triple staining immunofluorescence images were acquired separately in the green, red, and UV channels at a resolution of 102 x 1024 pixels, with the confocal pinhole set to one Airy unit, and then saved in TIFF format.

3.5.4 Protein extraction and Western blotting analysis

The expression of α-SMA was evaluated in the spheroids cultured for 96 h and 216 h on agar and for those cultured for 96 h and 216 h on agar and reverted to adhesion growth for twelve days. Cell collection, total protein extraction and Western blotting were performed as described in the paragraph 3.4.6. GAPDH was used as loading control.

3.6 Statistical analysis

All numerical data are presented as mean±SEM and were reported in Kaleida Grafh 4.0. Statistical differences between groups were evaluated with Student's two-tailed unpaired t-test; $p< 0.05$ was considered significant. For multiple comparisons, data were analyzed with one-way ANOVA with Bonferroni corrections. If not specified differently, data shown represent the means of three independent experiments.

Chapter 4

RESULTS

4.1 Analysis of primary cells from skin of neck

We have first carried out the morphological analysis of cells obtained from normal skin of neck, as reported in Material and Methods. To this aim, the presence of intermediate filaments and stress fibers was evaluated in monolayer cells by vimentin immunofluorescence and phalloidin staining, respectively (*Figure 5*). The analysis revealed the presence of vimentin intermediate filaments and stress fibers, which are cytoskeletal markers of mesenchymal cells such as proto-myofibroblasts [17], in the spindle-shaped cells. These cells were successively used for the preparation of spheroids.

4.2 Fibroblast three-dimensional cultures

4.2.1 Preparation

To begin with, we attempted to optimize standard techniques in order to ensure the formation of spheroids that are homogeneous in size at each different timepoint and that can be easily cultivated and finally collected for long-term experiments. For this aim, we have adapted the hanging-drops and agarose-coated U-bottom multi-well plates methods to generate spheroids *(Figure 6A)* [96]. Following the seeding, fibroblast aggregates formed after 24h of incubation, even if homogeneously sized 3D-spheroids with final tight form were seen only after 48h (*Figure 6B)*. Spheroid diameters were thus measured at 48h and 96h. The values at 48 h ranged from 471 μm to 528 μm with a mean volume of 0.065 mm^3 ± 0.004; at 72 h from 447 μm to 489 μm, with a mean volume of 0.053 mm^3 ±

0.003; at 96 h from 426 μm to 446 μm with a mean volume of 0.043 mm^3 ± 0.003. The volume of spheroids during their maturation decreased significantly after 96 h, possibly due to a compaction process. Indeed, with time, spheroids did not undergo a decomposition process and became more compact.

4.2.2 Vimentin immunohistochemical analysis

Immunohistochemical analysis of paraffin-embedded sections of spheroids collected at different times showed positivity for vimentin in all spheroids *(Figure 7)*. These results demonstrated that spheroids collected at the different time points are formed by cells preserving their mesenchymal origin [101, 102].

4.2.3 Evaluation of apoptotic cell death

DNA fragmentation represents a characteristic hallmark of apoptosis that can be evaluate by the TUNEL assay. The DNA strand breaks are detected by enzymatically labeling the free 3'-OH termini with modified nucleotides [103]. These new DNA ends are typically localized in identifiable nuclei and apoptotic bodies. In contrast, normal or proliferative nuclei usually are not stained as they contain insignificant numbers of DNA 3'-OH ends TUNEL was performed on sectioned spheroids collected at different times, to evaluate if the forcing of adherent cells, such as fibroblasts, to grow as multicellular aggregates could trigger apoptotic cell death *(Figure 8)*. The analysis evidenced only few nuclei positive for DNA strand breaks at all time points (2,3 % at 24 h, 1,7 % at 48 h, 0,5 % at 72 h and 0,2 % at 96 h). These results demonstrated that fibroblast clustering did not induce a massive apoptotic cell death.

4.2.4 Evaluation of necrosis markers

Haematoxylin and eosin staining was performed to evaluate the presence of necrosis based on the typically increased eosinophilia of the necrotic cells. The analysis did not detect any evident necrotic area in spheroids collected at different timepoints *(Figure 9*).

It is well known that during necrosis, loss of membrane integrity leads to cellular LDH release [38]; hence, we measured LDH enzymatic activity in conditioned media from fibroblasts grown either as monolayers or as spheroids, collected at indicated time points (*Figure 10).* Marginal levels and the comparable LDH activity were observed in conditioned media of both cultures. In particular, a significant increase of LDH activity was detected only after 96h of culture in the conditioned medium from both types of fibroblast culture, more evident in monolayer-conditioned medium.

4.2.5 Evaluation of inflammation and activation markers

To evaluate the levels of inflammation and activation markers specific of fibroblasts clustering and activation [38, 104], the levels of COX-2 and α-SMA proteins were analyzed in extracts of cells grown in monolayer and in spheroids collected at different timepoints.

Western blot analysis showed both the absence of COX-2 protein induction and the time dependent reduction of α-SMA levels in spheroid protein extracts *(Figure 11A).* In particular, the densitometric analysis demonstrated a time-dependent decrease of α-SMA levels starting at 48 h and becoming even more evident at 72 and 96h (*Figure 11B)*. This decrease of the specific myofibroblast marker α-SMA in spheroids suggests that myofibroblasts underwent a deactivation process during spheroid formation. Furthermore, the expression of α-SMA in monolayer cell protein extracts (*Figure 11B)* together with the

presence of vimentin intermediate filaments and stress fibers (*Figure 5B)*, previously shown, demonstrated that fibroblasts cultured as monolayer are myofibroblasts [17].

It is known that activated fibroblasts enhance the proliferation and motility of normal and cancer cells through paracrine interactions [105]. Therefore, the viability and migratory capability of non-tumorigenic keratinocyte (HaCat) and fibrosarcoma metastatic (HT1080) cell lines treated with either monolayer- or spheroid-conditioned medium were analysed by MTT and scratch wound assay, respectively [106]. The MTT assay showed that the viability of both cell lines incubated with spheroid-derived conditioned medium was lower when compared with cells treated with monolayer culture-conditioned medium *(Figure 12).* In particular, HaCat and HT1080 cell lines showed a reduction in cell viability of about 32% and 25%, respectively.

As shown in figure 13, the wound healing ability of HaCat cells treated with spheroid-conditioned medium was dramatically reduced compared to that observed in the same cells treated with monolayer-conditioned medium. In particular, at 24h after wounding, the quantitative analysis indicated a percentage of open surface area in HaCat culture containing spheroid-conditioned medium of about 44%. Conversely, at the same timepoint, in HaCat culture treated with monolayer-conditioned medium the scratch area was completely closed. On the other hand, HT1080 cells treated either with monolayer or spheroid conditioned medium showed a similar migratory capability, as the scratch wound was closed within 24h *(Figure 14).* Only in one of the three independent experiments, the wound was still opened, and it contributed to an elevated standard error in quantitative analysis. Hence, further experiments will be needed to better understand wound healing capability of HT1080 cells. The results of this experiment also suggested a noteworthy inhibitory effect of spheroid-conditioned medium on the growth of HT1080

cells. Taken together, these data indicate that myofibroblasts underwent a deactivation process in the spheroids.

Previous works showed that myofibroblastic activated phenotype is associated with increased secretion of growth factors, such as HGF [107], that support the proliferation and migration of normal and tumorigenic cells [2, 33, 44]. In our study, no significant differences in HGF concentration were detected between myofibroblast spheroids- and monolayers-conditioned medium, as evaluated by ELISA assay (not shown). Hence, the observed differences in cell survival and migration seem to be not dependent on HGF, even if further studies will be useful to clarify this issue.

4.2.6 Cell growth fraction evaluation

Ki-67 is a widely used cellular marker of proliferation and its expression was analyzed by immunohistochemistry on paraffin-embedded sections of spheroids collected at different timepoints *(Figure 15).* The analysis revealed the presence of about 6% of nuclei positive for Ki-67 in spheroids collected at 24h. It is important to specify that Ki-67 immunostaining, in all sections tested, did not localize in a restricted area but was evident in the centre as well as in the peripheral areas of the spheroids. At 48 hours, there were less than 1% of Ki67-positive nuclei and there were no positive cells after this time point.

4.3 Reversion of spheroids to adhesion and monolayer growth

Spheroids grown on agar for 96h and 216h were transferred to standard culture dishes or glass coverslips, to allow cell adhesion and spreading and to analyse spheroids during possible reversion to monolayer growth. This analysis demonstrated that spheroids can revert to monolayer growth *(Figure 16)*.

4.3.1 Evaluation of cell cycle phases

A live cell detection colorimetric assay was used to evaluate cell cycle phases of monolayer cells derived from spheroids. This analysis showed that monolayer cells from spheroids collected at 96 h were in G0/G1, S, or G2/M phases *(Figure 16A)*. In the population of monolayer cells from spheroids harvested at 216 h, only rare cells were in S phase *(Figure 16B).*

4.3.2 Confocal immunofluorescence analysis

Confocal immunofluorescence analysis showed that cells of spheroids that were cultured for 96h on agar and reverted to adhesion growth for 12 days contained vimentin intermediate filaments and stress fibers *(Figure 17A)*. Cells of spheroids that were reverted to monolayer growth after 216h in agar displayed vimentin intermediate filaments but contained fewer stress fibers than spheroids collected at 96h *(Figure 17B)*. Moreover, in cells of spheroids collected at 96h the vimentin and phalloidin staining colocalization was evident.

4.3.3 Western blotting analysis

Western blotting of α-SMA showed a decrease of the protein expression in spheroids collected at 96h and 216h and reverted to monolayer growth, with respect to monolayer myofibroblasts *(Figure 18A)*. In particular, by densitometric analysis, this α-SMA reduction resulted particularly evident in extracts from spheroids collected at 216h and reverted to monolayer growth *(Figure 18B)*. Furthermore, there was not a significant difference in the α-SMA levels between spheroids grown on agar and spheroids reverted to monolayer growth after 216h of three-dimensional culture**.**

4.4 Clusters and spheroids formed spontaneously

Surprisingly, we found that, after 16 days, myofibroblasts from the skin of neck formed multicellular aggregates spontaneously, in the absence of agar, both in plastic 12-well plates or on glass coverslips *(Figure 19)*. In particular, fibroblast clustering and spheroid formation were observed when the cell cultures remained 100% confluent for several days.

Chapter 5

DISCUSSION

The organization and physiological functions of multicellular organisms depend, among other factors, also on the cues from the connective tissue [36]. Fibroblasts are versatile and heterogeneous connective tissue cells which can acquire an activated and immunoregulatory phenotype, characterized by *de novo* expression of α-SMA and production of large amounts of COX-2 and proinflammatory cytokines [54, 2]. The activation of fibroblasts is a process controlled by continuous chemical and mechanical changes of the tissue microenvironment, which coincide with fibroblast to myofibroblast differentiation. Fibroblast-to-myofibroblast transition begins with the formation of the proto-myofibroblasts, containing stress fibres with β- and γ-cytoplasmic actins, and continues as they transform into myofibroblasts that present stress fibres with α-SMA [33]. α-SMA in stress fibres is the most commonly used molecular marker for myofibroblasts, and confers to these cells a stronger contractile function compared to proto-myofibroblasts [22, 23]*;* instead the mesenchymal intermediate filament protein vimentin is a common marker for fibroblasts and myofibroblasts [108]. The myofibroblasts have been identified both in physiological conditions, where there is a necessity of mechanical force development for the rapid repair of damaged tissues, and in pathological conditions, such as fibrotic tissues and cancer [17]. To the best of my knowledge, this is the first study that combines these two factors, i.e. the use of primary fibroblasts and the cluster formation. In this study, we generated and analysed clusters, namely spheroids, of human primary cutaneous myofibroblasts. In comparison with the

established fibroblast clusters, the clusters of human primary fibroblasts better represent the stromal microenvironment.

It is known that fibroblasts *in vitro* differentiate to myofibroblasts when cultured on high stiffness substrate, such as plastic dishes, in the presence of TGF-β [17]. Moreover, Santiago *et al*. demonstrated that fibroblasts, cultured on standard plastic plates, express α-SMA and differentiate to myofibroblasts [109].

The monolayer myofibroblasts used to generate spheroids also express COX-2 protein; in particular, it has been demonstrated by a previous study that COX-2 mRNA can be induced by fetal bovine serum [110]. Furthermore, it is known that the fetal bovine serum, present in monolayer and spheroids culture medium, can activate a transcriptional program related to physiology of wound repair in human primary cultured fibroblasts [110].

Myofibroblast aggregates and nodules are observed in wound healing and hypertrophic scars, respectively [36]. The aggregates of fibroblasts were observed in the dermis at early stages of melanoma development, before metastasis formation. Moreover, there is a paracrine interaction between cancer cells and fibroblasts [76]. While at the end of wound healing, the activated fibroblasts undergo apoptotic cell death, the same cells *in vitro* endure a programmed necrosis-like cell death, called nemosis, associated with COX-2 induction and inflammatory response [2, 37]. During inflammation, wound healing and cancer, fibroblasts can lose their contacts to ECM. In these conditions several proteases, destroying ECM structure, liberate fibroblasts from ECM and trigger fibroblasts clusters formation [16]. These differences in biological cell characteristics and behaviour *in vivo* and *in vitro* represent a major hurdle in the studies of the activated fibroblast role in wound healing and cancer development. Aiming at overcoming this obstacle, we generated spheroids using and modifying the previously described hanging-drops and agarose-coated U-bottom well plates methods [96]. Such growth of fibroblasts can reflect

in vivo conditions, with the fibroblasts loosing their contact with the connective tissue, allowing the studies of myofibroblast turnover and contribution to organ remodelling.

The present study demonstrated that human primary myofibroblasts from normal skin of neck can be induced to grow as multicellular aggregates, leading to myofibroblasts deactivation. Such approach to myofibroblast culture and analysis could represent an experimental model to study myofibroblast and tissue turnover. The results of the study demonstrated that human primary myofibroblasts, if forced to grow as multicellular aggregates, preserve their mesenchymal characteristics and do not undergo apoptosis or nemosis. In particular, we showed that cell clustering did not lead to induction of COX-2 protein that is associated with inflammatory response [38]. Furthermore, the significant α-SMA protein expression decrease in spheroids collected at different timepoints suggested that three-dimensional aggregation of myofibroblasts induced a deactivation process. Analysis of spheroids reverted to monolayer growth demonstrated that this deactivation process is reversible for spheroids collected at 96h and seems to be only partially reversible for spheroids collected at 216h. In particular, phalloidin staining showed that cells of spheroids collected at 216h developed stress fibres less extensively than spheroids collected at 96h. Moreover, the significant difference of α-SMA levels, detected between spheroids reverted to monolayer growth after 96h and 216h of three-dimensional culture, confirms and explains the immunofluorescence analysis. Therefore, the morphological and molecular phenotype of spheroids collected at 216h resembles proto-myofibroblasts phenotype. The vimentin and phalloidin staining colocalization detected in spheroids at 96h is in agreement with previous studies showing that stress fibres contain vimentin [111] and that actin and vimentin filaments can interact directly [112].

Paracrine epithelial-mesenchymal cell interactions play important role in both tissue repair and cancer progression [14, 105], indeed activated fibroblasts support the proliferation and migration of normal and tumorigenic cells [2, 33]. In particular, previous studies showed that conditioned medium of activated fibroblasts triggers the proliferation and migration of non tumorigenic and tumorigenic cell lines, by increasing the expression of growth factors such as HGF/SF [105, 113, 114]. HGF/SF is a potent multifunctional growth factor produced by mesenchymal cells, with fibroblasts being its primary source [115]. HGF/SF has high affinity for the receptor tyrosine kinase c-Met [44]. In particular, HGF/SF induces Met signalling pathways regulating multiple cellular responses, such as migration, invasion, proliferation, branching morphogenesis, angiogenesis, mitogenesis and cancer cells tumorigenesis [116, 117, 118]. During wound healing, both migration and proliferation of keratinocytes are required for the re-epithelization [119]. Proliferation and motility are also two key features for tumor progression. Motility is needed for the dissemination from the site of primary tumor, leading to invasive phenotype [47]. Cancer progression shows striking similarities with wound healing, since it also requires epithelial-mesenchymal interactions [45]. Furthermore, the tumor microenvironment, and in particular the role of activated fibroblasts, has been shown to be an important contributor to the tumor progression [13]. On this basis, we decided to investigate how inactivated fibroblasts within spheroids influence the behavior of the HaCat and HT1080 cells with regard to their proliferative and migratory response. Of note, HaCat and HT1080 are both c-Met positive cell lines [2, 120]. It is known that wound healing in HaCat cells is a combination of cell proliferation and migration [105]. Hence, these cell properties were evaluated in our study. First, we detected a cytostatic effect exerted by the spheroid-conditioned medium on both normal and cancer cell lines in MTT assay; this observation confirmed the deactivation of

myofibroblasts inside spheroids. Next, the wound healing assay demonstrated that spheroid-conditioned medium significantly delays the HaCat wound closure. Conversely, HT1080 cells treated with monolayer- or spheroid-conditioned medium displayed a similar migratory capability. Moreover, spheroid-conditioned medium seemed to inhibit the growth of HT1080 cells. Indeed, it is known that HT1080 proliferation and migratory capability can be differently regulated [121].

Our preliminary data showed that there are not differences in HGF/SF secretion levels between myofibroblasts forming monolayer and spheroids. Hence, these data call upon an in-depth examination of the paracrine interactions between spheroids and tumor cells. Indeed, it remains unknown whether the observed cytostatic and anti-migratory effect is due to toxic compounds present in spheroid-conditioned medium or it is associated with paracrine interactions mediated by other growth factors or by vesicles such as exosomes.

Ki-67 is used as the marker of proliferation and it is expressed in cells committed to the progression through cell cycle and thus during late G1, S, G2, and M phases, but not in resting cells in G0 [122]. In this study, deactivation of myofibroblasts inside spheroids is further supported by Ki-67 staining analysis. In particular, immunohistochemical analysis of Ki-67 showed that after 48h of tridimensional culture there were no positive nuclei for Ki-67 and all cells were in G_0 cell-cycle phase. Furthermore, the presence of positive nuclei for Ki-67 in spheroids collected after 24h suggests that fibroblasts do not stop proliferating abruptly during spheroids formation and that, as also shown by the time-dependent decrease of α-SMA protein levels, myofibroblasts deactivation is a step-by-step process.

For many years, myofibroblast differentiation was considered irreversible process; therefore myofibroblasts were believed to be terminally-differentiated cells. As observed in several studies [37, 42, 123], at the end of wound healing, myofibroblasts undergo programmed cell death. To date it is not clear if myofibroblasts can acquire an *in vivo*

stable inactivated phenotype. In the present study, colorimetric evaluation of cell-cycle phases of spheroids reverted to monolayer growth demonstrated that fibroblasts maintained their proliferation capability within spheroids. Hence, the spheroid can be seen as a cell reservoir able, when needed, to liberate fibroblasts that can be re-activated. Similar conclusions emerge from other studies indicating that myofibroblasts can revert to a non-activated phenotype [123]. In particular, it was shown that murine myofibroblasts, originated from hepatic stellate cells, could revert to inactive phenotype during regression of liver fibrosis: these deactivated cells can be rapidly reactivated into myofibroblasts in response to fibrogenic stimuli [124].

It is intriguing that we observed spontaneous spheroid formation on high stiffness substrates represented by plastic or glass culture ware. Supposedly, this cluster formation could be a physiological and intrinsic feature of cutaneous myofibroblasts. Furtherrmore,it would be interesting to analyse these spontaneous spheroids and to compare them with spheroids generated on agar.

Chapter 6

CONCLUSIONS

During the last years, important advances have been made in the understanding of several aspects of myofibroblast biology. Fibroblasts are highly heterogeneous mesenchymal cells with the capability to acquire an activated phenotype. This activation is represented by their differentiation into myofibroblasts, a process that occurs in wound healing and cancer. In particular, once the wound is repaired, the number of activated fibroblasts decreases significantly as they undergo apoptosis. It is not known whether the myofibroblasts apoptosis is followed by tissue repopulation through fibroblasts from adjacent tissue [17]. Moreover, the hypothesis that activated fibroblasts can revert to an inactivated phenotype is controversial because they have been always believed terminally differentiated cells.

This "dogma" is subverted by our data that support recent works sustaining that activated fibroblasts can revert to inactivated phenotype. As a matter of fact, we not only showed that *in vitro* human primary myofibroblasts from skin can be induced to grow as multicellular aggregates and do not die by apoptosis or nemosis, but we also documented that these cells undergo reversible deactivation during spheroids formation.

The investigations on the reversibility of the myofibroblast differentiation are particularly important for the treatment of diseases involving myofibroblasts that do not undergo apoptotic cell death but remain constitutively activated. Our results support the use of 3D cultures in biomedical research to bridge the gap between traditional cell cultures and *in vivo* settings in order to more clearly understand the inactivation mechanisms and

turnover of myofibroblasts. Accordingly, the approach introduced in this study could represent a tool for analysing the morphological and molecular mechanisms leading to myofibroblasts inactivation. Although further investigations are necessary, the current evidence shows that is conceivable that this experimental system might serve as a new important tool for studying several myofibroblast-related diseases, such as cancer, and could contribute to the development of new therapeutic strategies. One possible implementation of the deactivated fibroblast microenvironment present within spheroids is that its components could be able to inhibit tumor cell proliferation without inflammatory processes. In this perspective, *in vivo* studies should be employed in order to evaluate and validate this hypothesis.

Chapter 7

ICONOGRAPHY

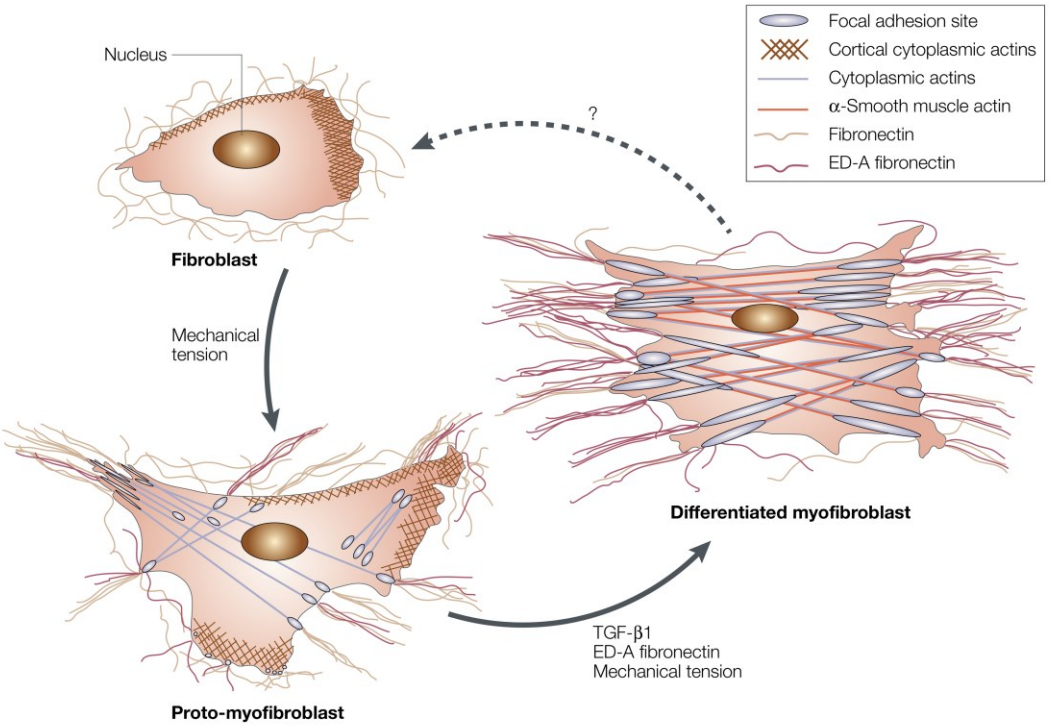

Tomasek et al. 2002, Nature Reviews Molecular Cell Biology

Figure 1

Fibroblast differentiation. Fibroblasts contain actin microfilaments organized predominantly into their cortical meshwork but do not show stress fibers and present fibronectin excluding ED-A segment. Under mechanical stress, fibroblasts will differentiate into proto-myofibroblasts, which form cytoplasmic actin containing stress fibres. Additionaly, proto-myofibroblast express fibronectin including the ED-A splice variant. Transforming growth factor β1 (TGF-β1) increases the expression of ED-A fibronectin and together, in the presence of mechanical stress, promote proto-myofibroblasts into myofibroblasts differentiation. Myofibroblasts contain stress fibers represented by the *de novo* expression of alpha smooth muscle actin (α-SMA), their most reliable marker, and supermature focal adhesions. Myofibroblasts have a greater contractile force than proto-myofibroblasts.

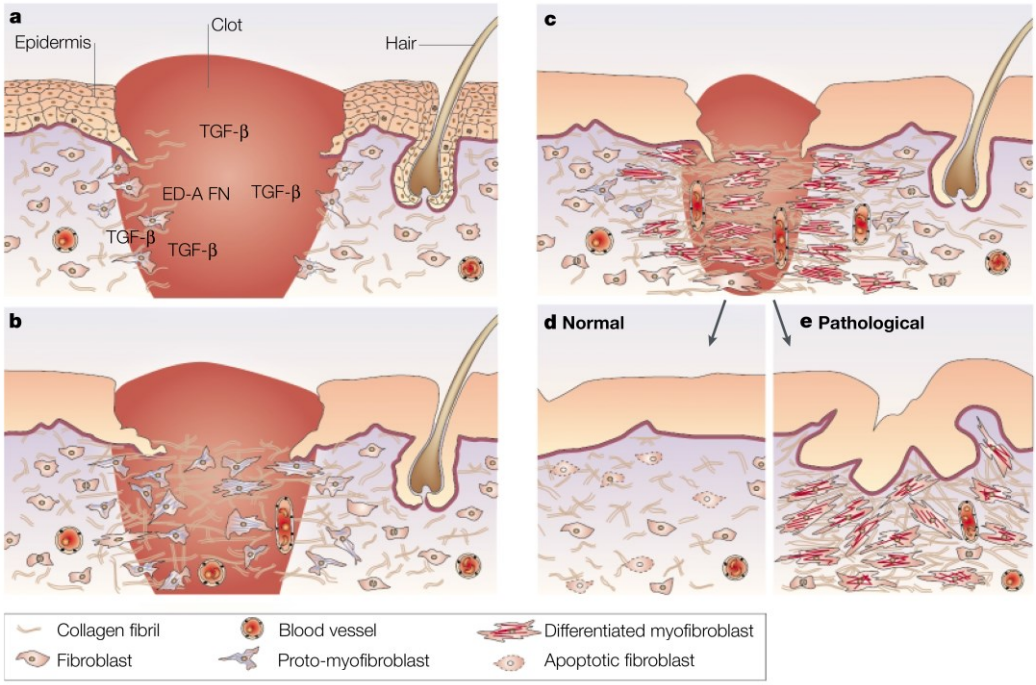

Tomasek et al. 2002, Nature Reviews Molecular Cell Biology

Figure 2

Model of the role of myofibroblasts during wound healing. (A) In normal tissues, fibroblasts are inactivated and do not present developed contractile apparatus. When a full-thickness dermal wound is filled by a fibrin clot, local growth factors stimulate fibroblasts from the adjacent intact dermis to intervene. They invade the provisional matrix, fill the wound formating the granulation tissue. (B) Migrating fibroblasts exert tractional forces on the collagen matrix and this mechanical stress stimulates fibroblasts to develop stress fibres and to produce collagen. Fibroblasts acquire the proto-myofibroblast phenotype and secrete transforming growth factor β1 (TGF-β1) and increased levels of ED-A fibronectin (ED-A FN). (C) Proto-myofibroblasts become differentiated myofibroblasts by synthesizing α-SMA. They generate increased contractile force and remodel the ECM, with the aim to close the wound. (D) When a normal healing wound closes, myofibroblasts disappear by apoptosis. (E) In many pathological situations, myofibroblasts persist and continue to remodel the ECM.

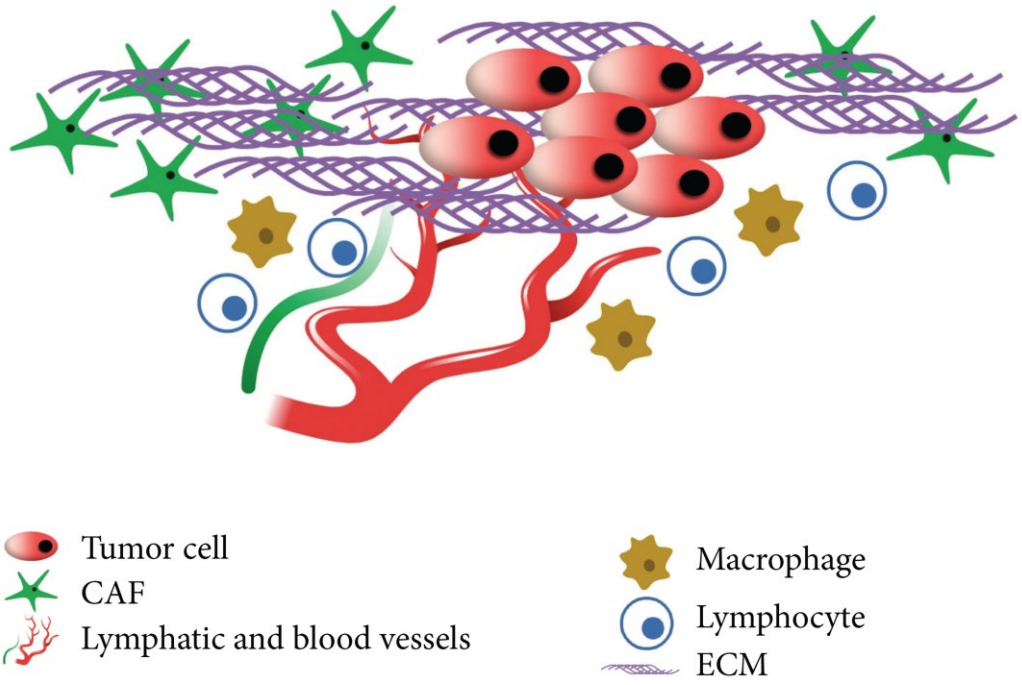

Arcucci et al. 2016, BioMed Research International

Figure 3

Components of solid tumors microenvironment. Cancer microenvironment includes blood and lymphatic tumor vessels, extracellular matrix (ECM), tumor cells and non cancer stromal cells such as endothelial cells, immune cells and cancer associated fibroblasts (CAFs).

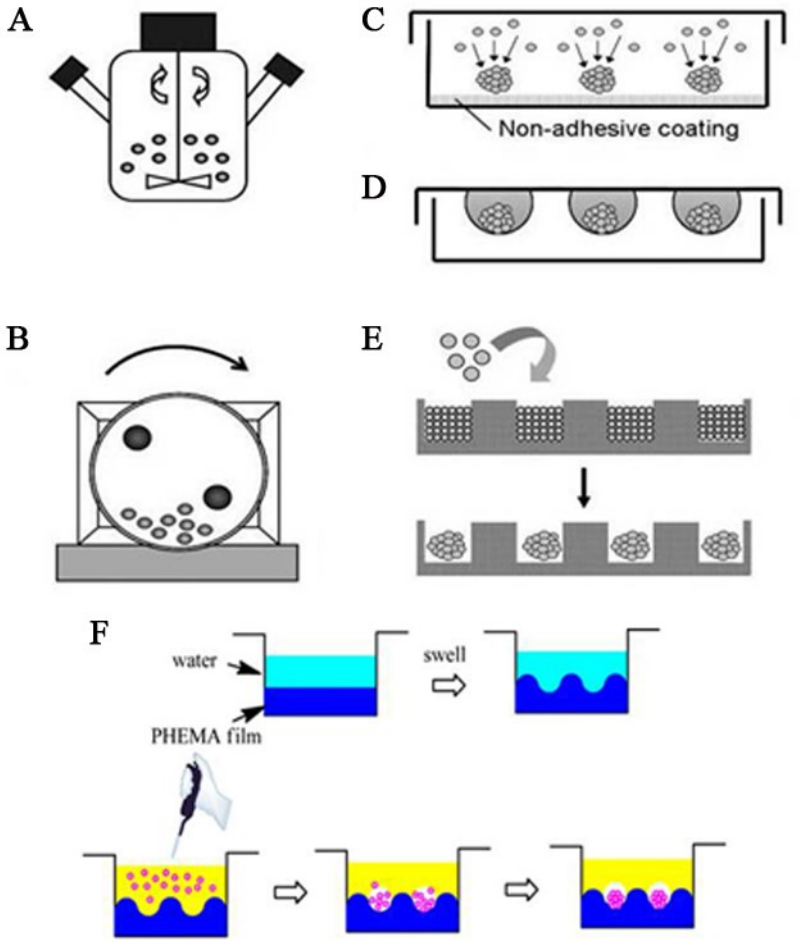

Lin et al 2008, **Biotechnology Journal**
Zhao et al 2014, **Biomacromolecules**

Figure 4

Methods for spheroid generation. (A) Spinner flask culture. (B) Rotary cell culture systems. (C) Cell culture on adhesive surface. (D) Hanging-drop culture. (E) Micromolding techniques. (F) Swelling-induced wrinkling patterns culture.

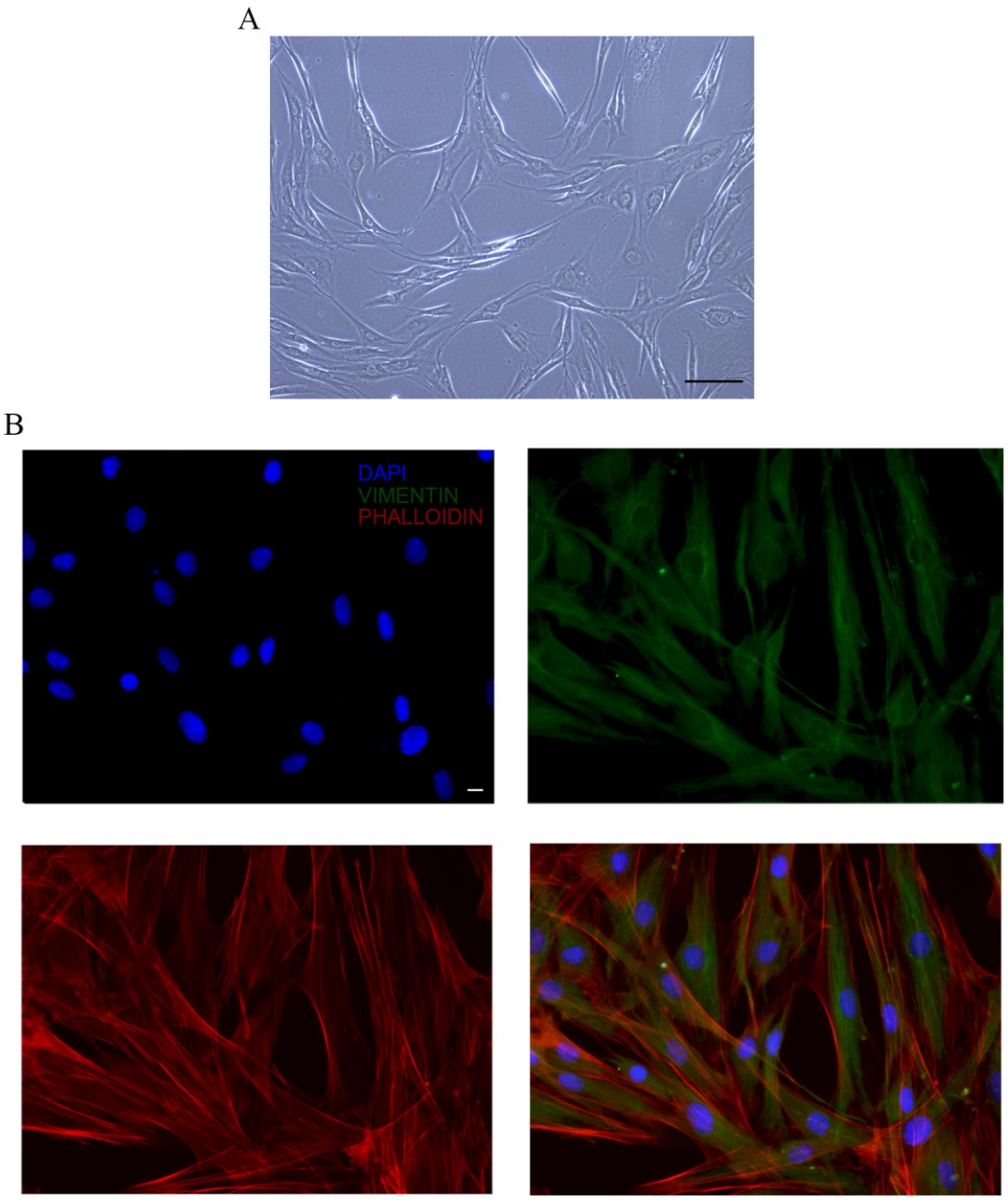

Figure 5

Primary human cutaneous fibroblasts. (A) Representative image of fibroblast cells obtained by outgrowth from explants of normal neck skin. Scale bar 100µm. Magnification X10. (B) Vimentin immunofluorescence (green channel) and phalloidin fluorescence (red channel) for morphological analysis of primary cells used to generate spheroids. DAPI (blue channel) was used to locate the nuclei. Scale bar 10µm. Magnification X40.

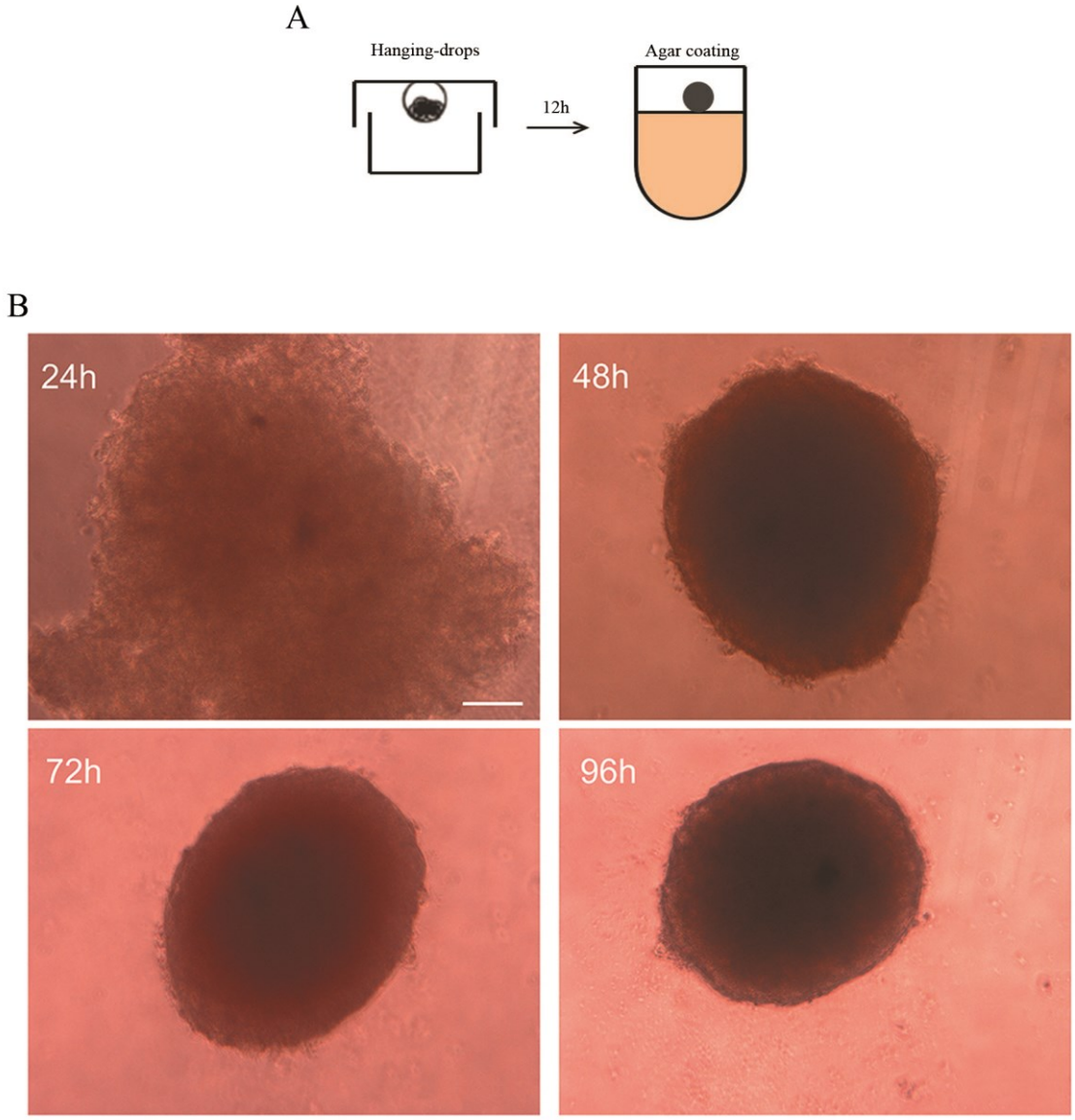

Figure 6

Method used for generating three-dimensional culture and clustering of the same spheroid. (A) Representative image of technique followed to obtain human primary fibroblast spheroids adapting the hanging-drops and coated plate methods (B) Photographs of the same spheroid during three-dimensional culture. Images were taken through phase contrast microscope at the indicated time points. Scale bar 100μm. Magnification X10. The images are representative of three independent experiments.

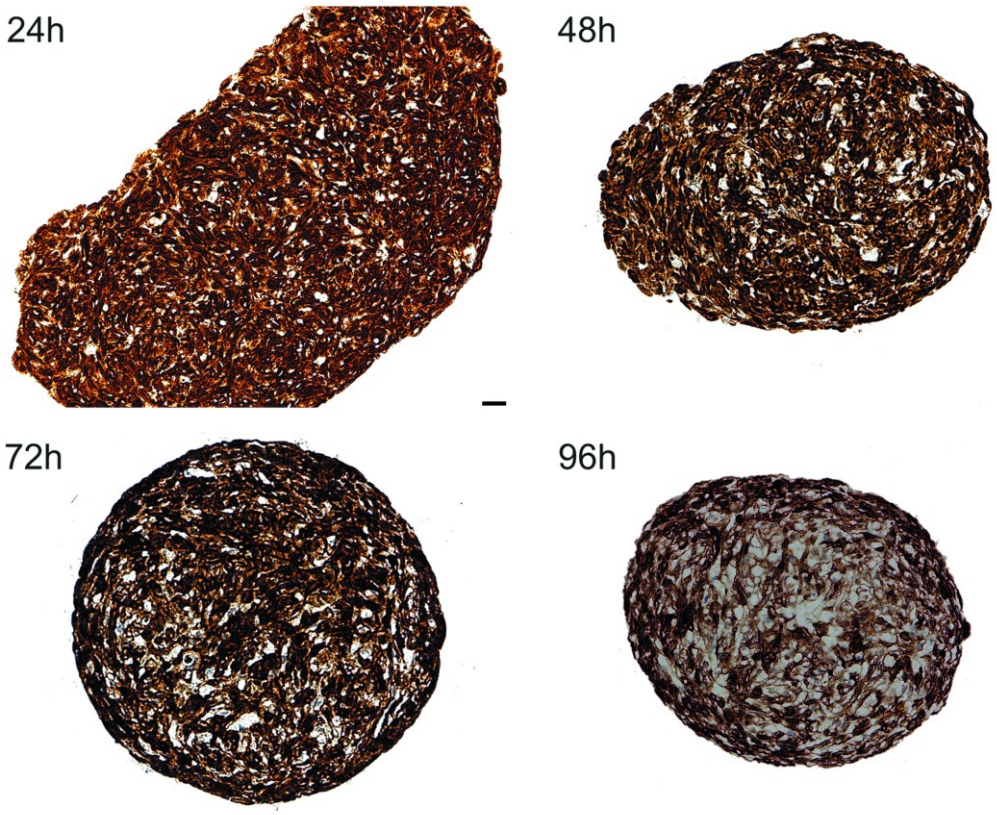

Figure 7

Vimentin immunohistochemical analysis. Vimentin immunohistochemical analysis of spheroids collected at indicated time points. Scale bar 25μm. Magnification X20. The images are representative of three independent experiments.

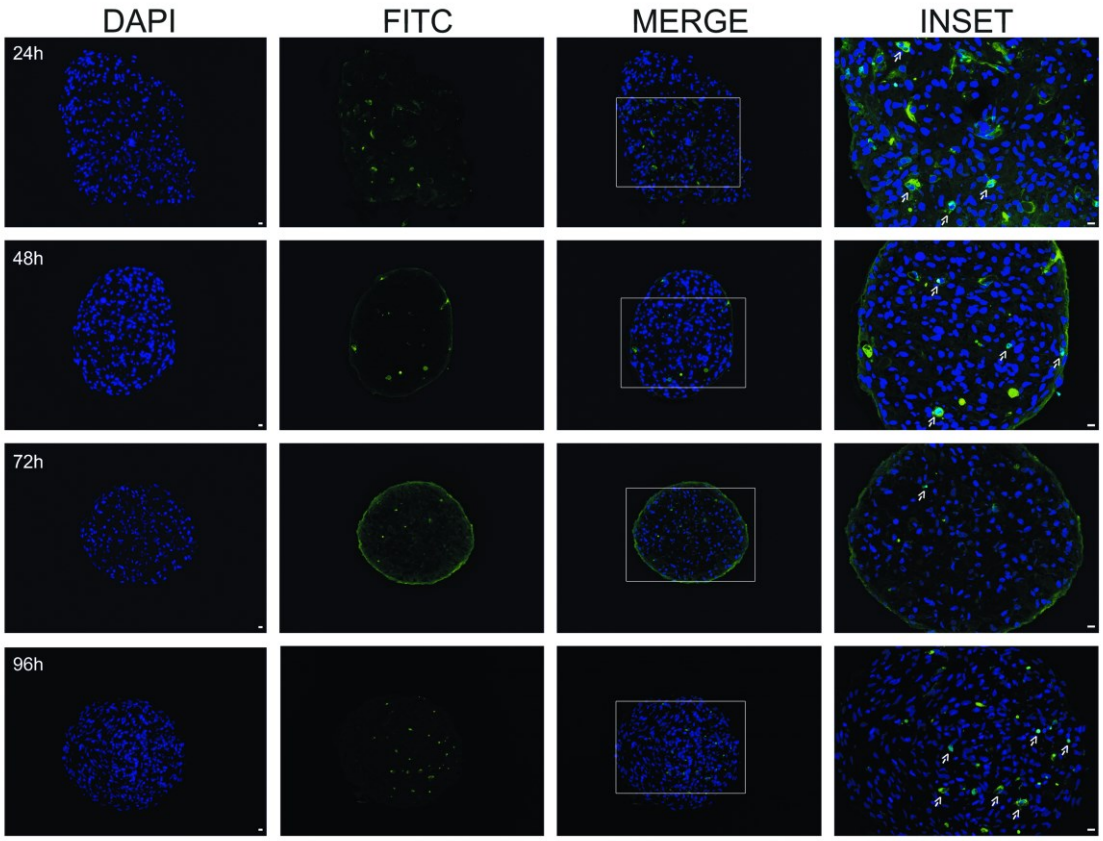

Figure 8

Evaluation of apoptotic cell death. TUNEL staining (green channel) of spheroids collected at indicated time points. DAPI (blue channel) was used to locate the nuclei. Scale bar 10µm. Magnification X10. INSET: Scale bar 10µm, Magnification X20. Apoptotic nuclei in the insets are indicated by arrows. The images are representative of three independent experiments.

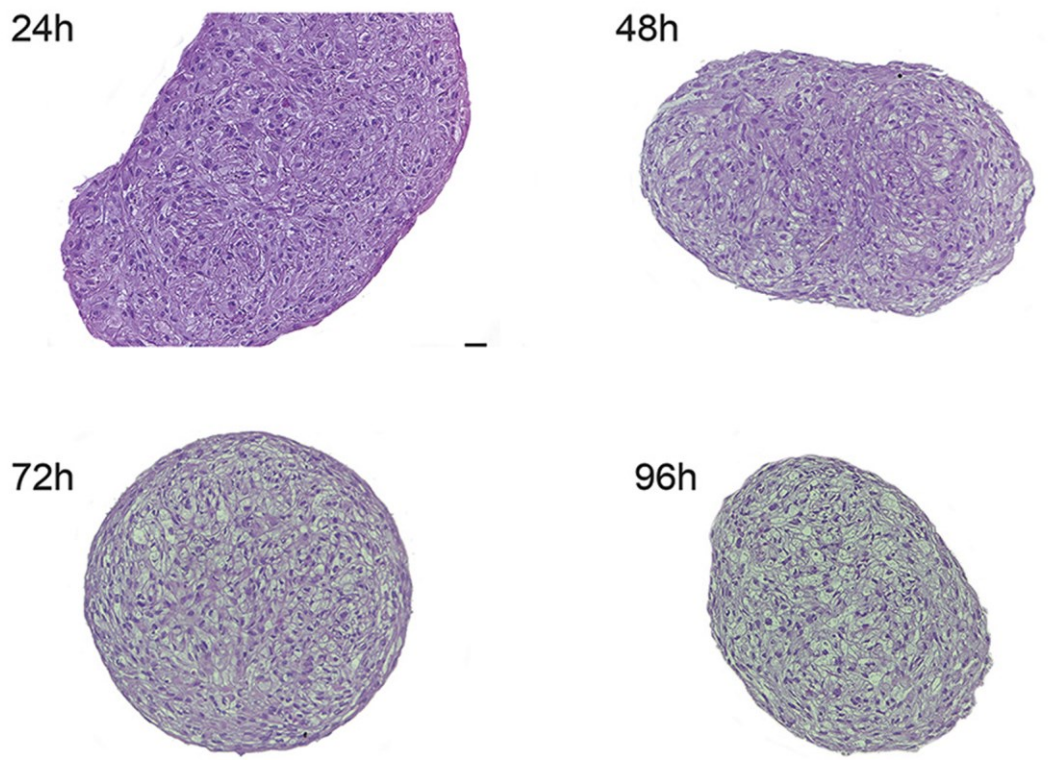

Figure 9

Evaluation of necrosis markers. Haematoxylin and eosin staining of paraffin-embedded sections of spheroids. Scale bar 25μm. Magnification X20. All images are representative of three independent experiments.

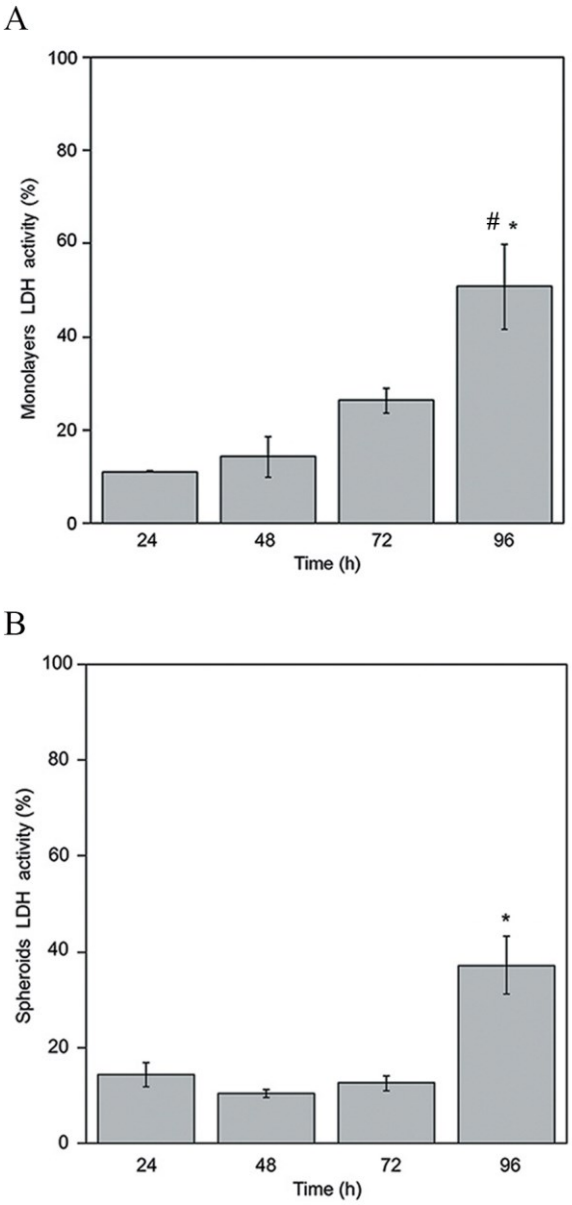

Figure 10

Evaluation of necrosis markers. At selected time points, necrosis was assessed by the measurement of the activity of LDH released in the conditioned medium of both monolayers (A) and spheroids (B). Data are means of three independent. experiments.(A) ± SE. #$p<0.005$ vs 24h and *$p<0.01$ vs 48h. (B) *$p<0.01$ vs 24h, 48h, 72h.

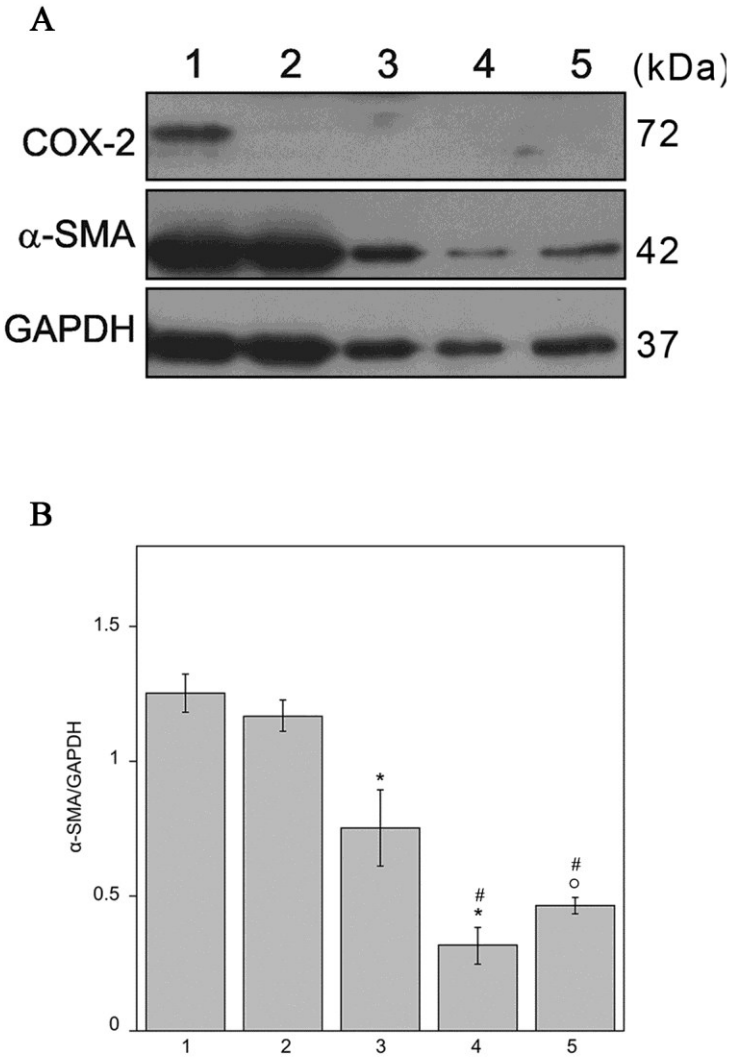

Figure 11

Evaluation of inflammation and activation markers. (A) Western blotting analysis of COX-2 and α-SMA. Protein extracts of fibroblasts monolayer (1), spheroids collected at 24h (2), 48h (3), 72h (4) and 96h (5). GAPDH was used as loading control. Representative image of three independent experiments is shown. (B) Densitometric analysis of α-SMA protein levels. Data are reported as mean of three independent experiments ±SE. *$p<0.05$ for 3 vs 1, 3 vs 2 and 4 vs 3; °$p<0.005$ for 5 vs 2; #$p<0.0005$ for 4 vs 1, 4 vs 2 and 5 vs 1.

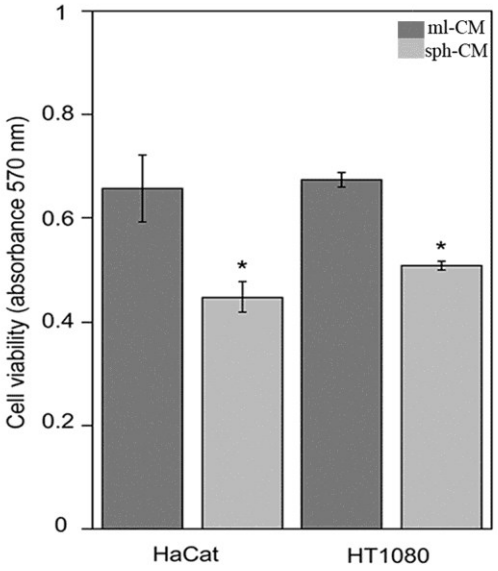

Figure 12

Effect of conditioned medium of fibroblasts monolayer (ml-CM) and spheroids (sph-CM) on normal and cancer cells. HaCat and HT1080 cells were grown for 48 h with conditioned medium and their cell viability was evaluated by MTT assay. Data are means of three independent experiments. ±SE.*$p<0.0001$.

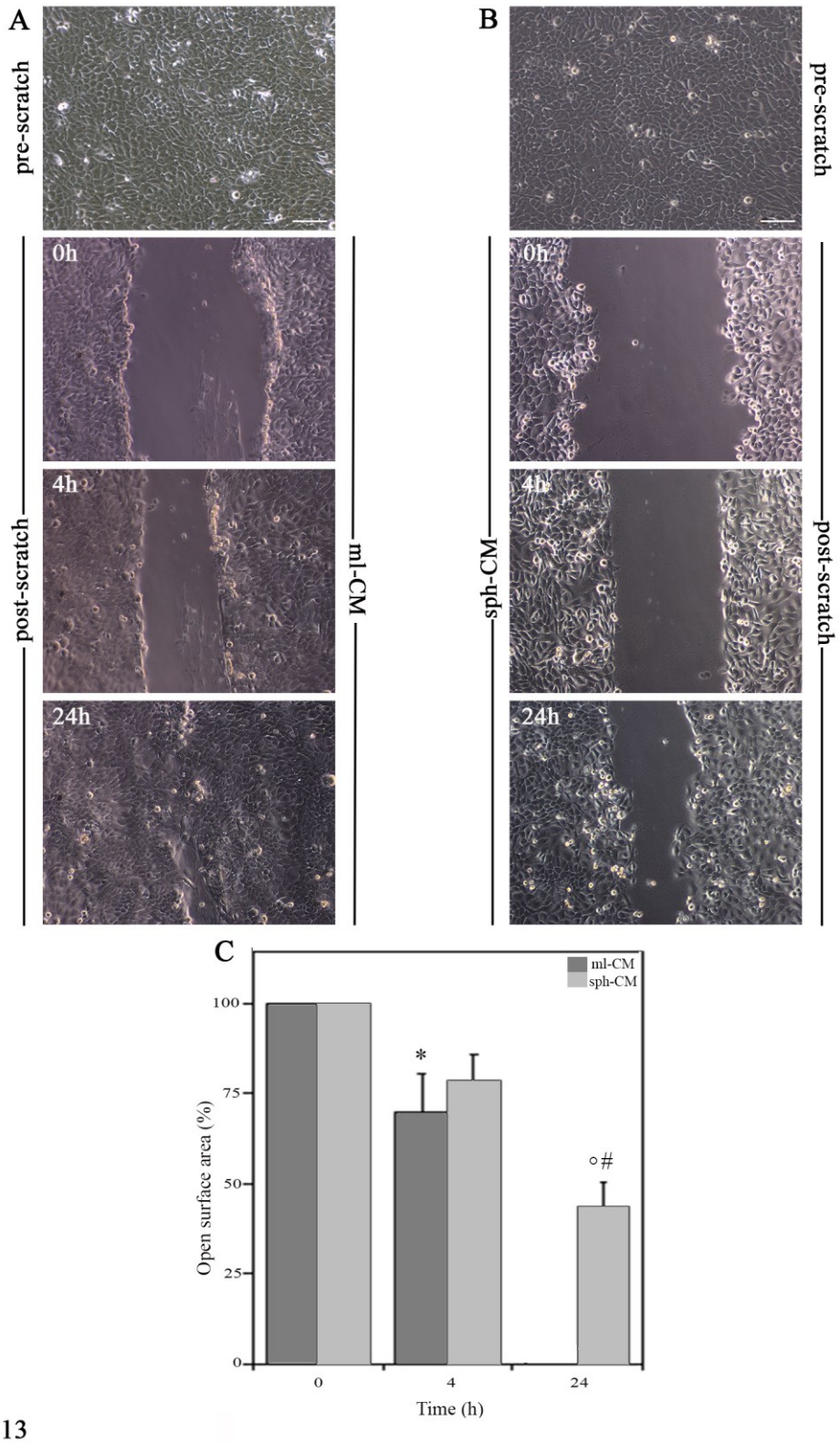

Figure 13

Wound healing assay. (A,B) Effect of monolayer (ml-CM) and spheroid (sph-CM) conditioned medium to HaCat wound healing. The representative images show the same fields before scratching and at 0h, 4h, 24h after wounding. Scale bar 100µm. Magnification X10. (B) Quantification of the wound healing assay. Wound widths were measured at indicated times. Data are expressed as the fold-decrease of area respect to control set as 100% and are reported as mean of three independent experiments. ±SE. *$p<0.05$ vs 0h; °$p<0.01$ vs 0h and #$p<0.005$ vs 4h.

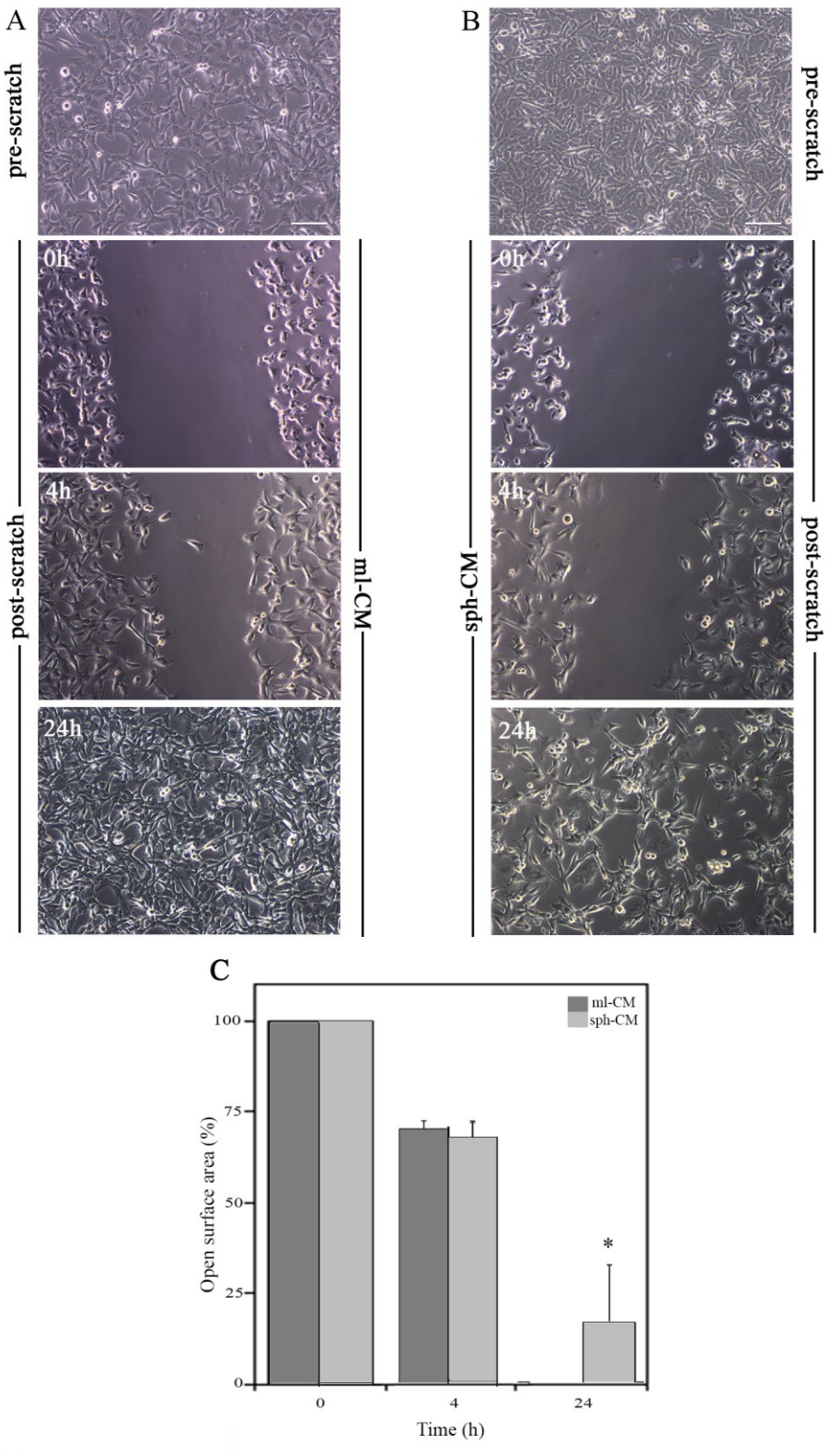

Figure 14

Wound healing assay. (A, B) Effect of monolayer (ml-CM) and spheroid (sph-CM) conditioned medium to HT1080 wound healing. The representative images show the same fields before scratching and at 0h, 4h, 24h after wounding. Scale bar 100µm. Magnification X10. (C) Quantification of the wound healing assay. Wound widths were measured at indicated times. Data are expressed as the fold-decrease of area respect to control set as 100% and are reported as mean of three independent experiments ±SE.*$p<0.005$ vs 0h and 4h

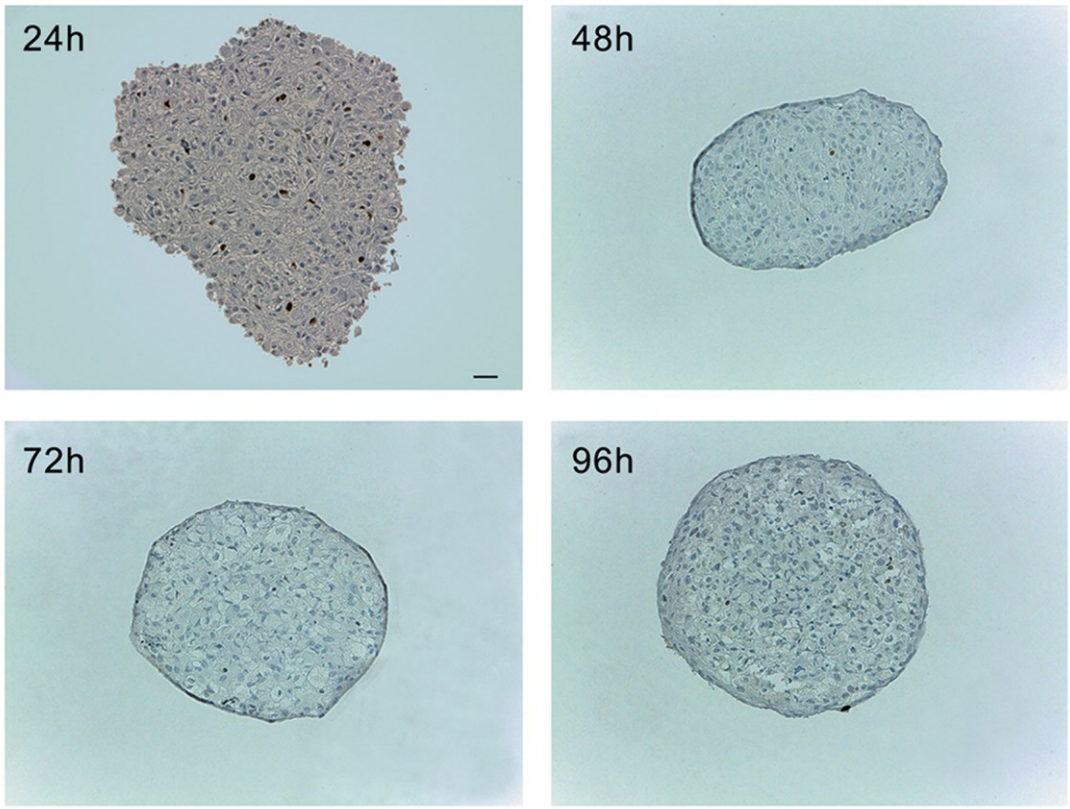

Figure 15

Ki-67 immunohistochemical analysis. Ki-67 staining of paraffin-embedded sections spheroids collected at indicated time points. Scale bar 25μm. Magnification X20. All images are representative of three independent experiments.

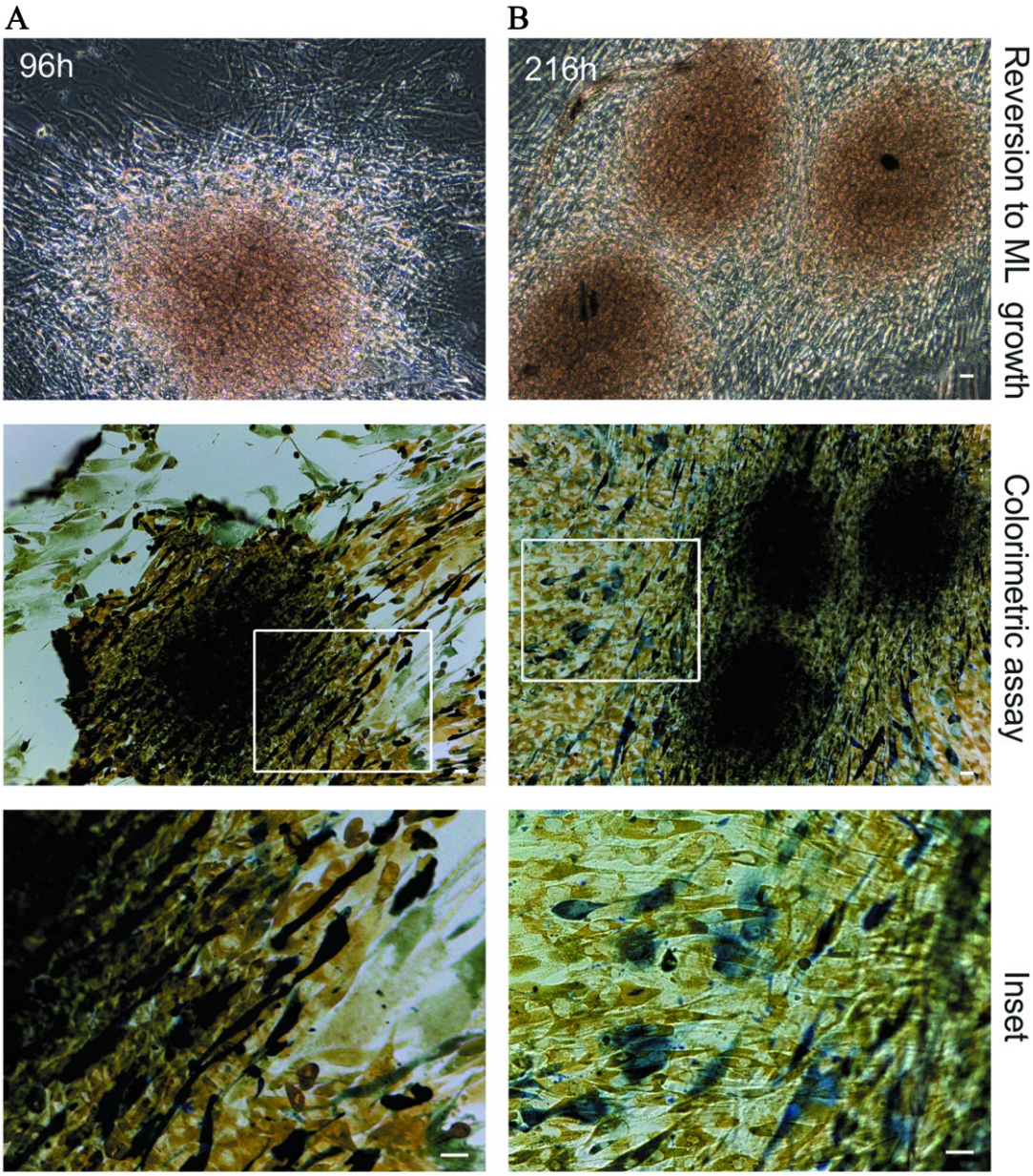

Figure 16

Analysis of spheroid reversion to monolayer growth. Images represent spheroids that were collected at 96h (A) and 216h (B) from agar and reverted to monolayer growth by transferring them onto plastic dishes; cells were maintained in culture for 12 days and then stained with a live cell detection kit to monitor cell cycle. Yellow pixels represent cells in G0/G1 phase, green pixels represent cells in S phase and dark blue pixels represent cells in G2/M phase. Scale bar 25µm. Magnification X10. Inset: Scale bar 25µm, Magnification X20. The images are representative of three ındependent experıments.

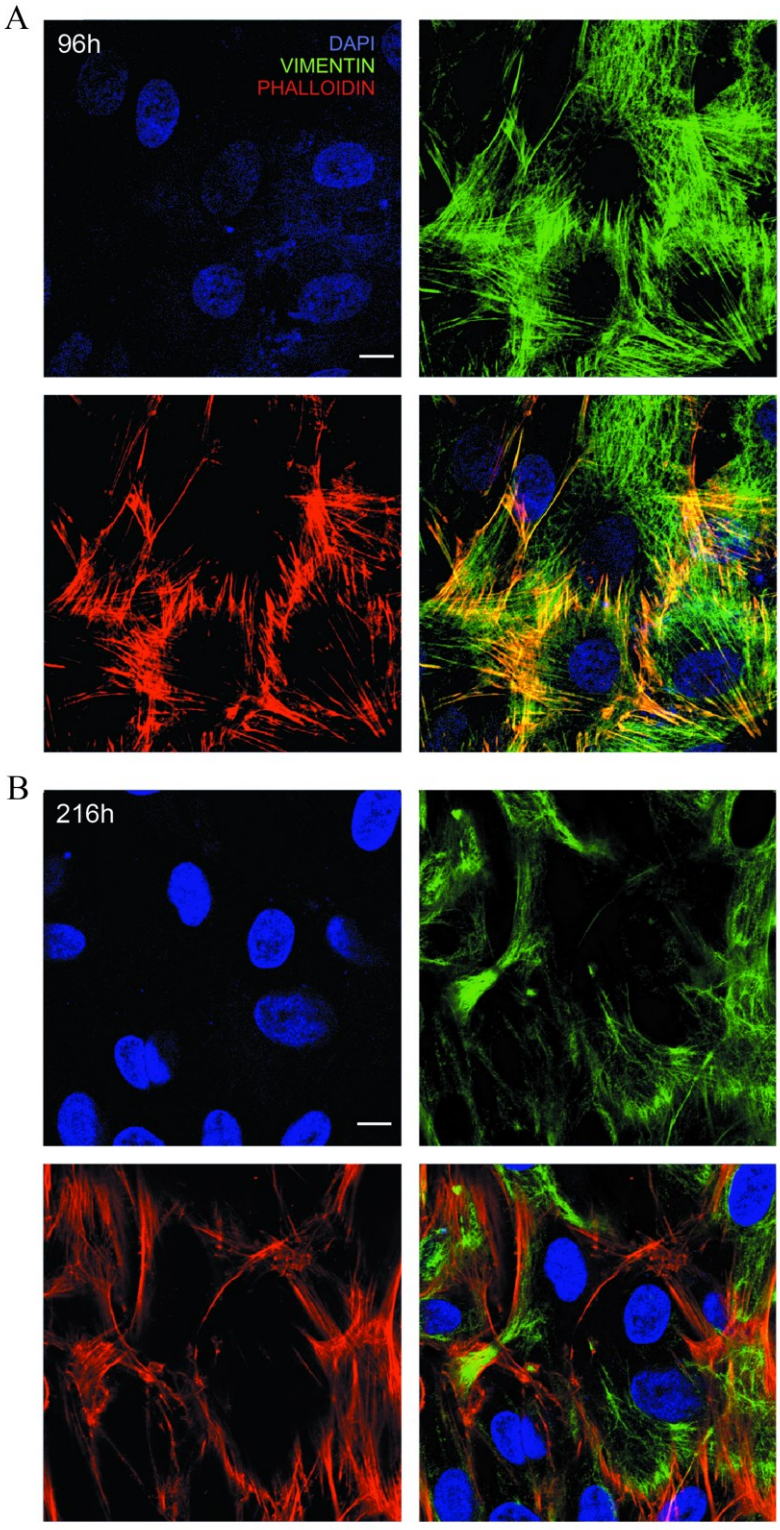

Figure 17

Immunofluorescence analysis of spheroids reverted to monolayer growth. Spheroids collected at 96h (A) and 216h (B) were transferred to glass coverslips and maintained in colture for 12 days. Images represent confocal analysis of vimentin immunofluorescence (green channel) and phalloidin staining (red channel). DAPI (blue channel) was used to locate the nuclei. Scale bar 10μm. The images are representative of three independent experiments.

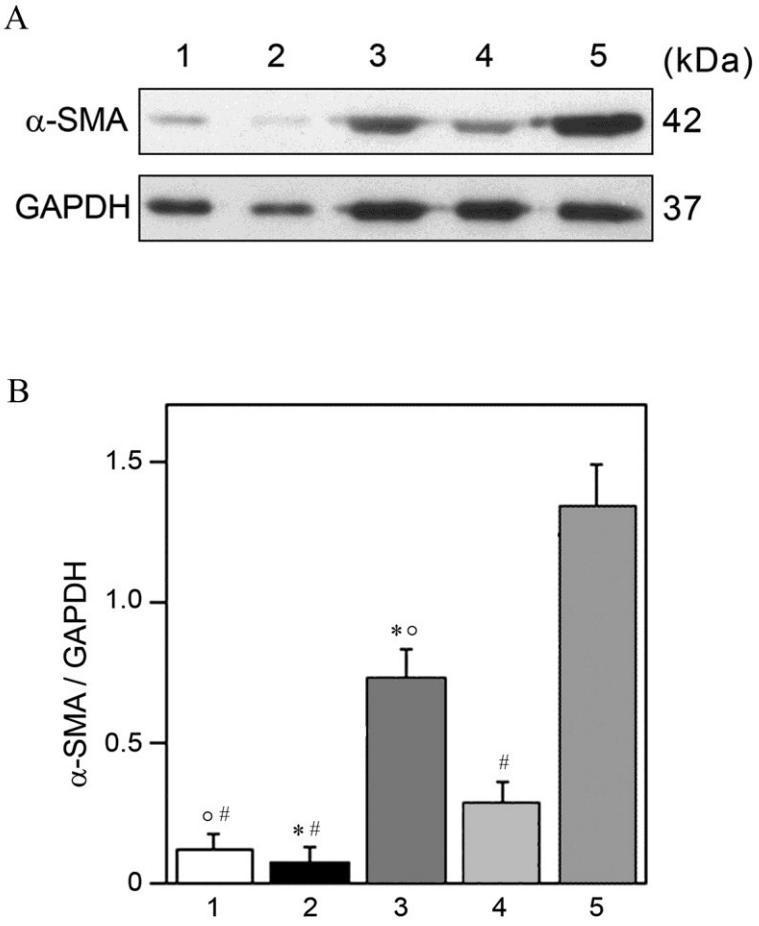

Figure 18

Evaluation of α-SMA expression. (A) Western blotting analysis of α-SMA in protein extracts of spheroids collected at 96h (1), 216h (2), spheroids reverted to monolayer growth after 96h (3), 216h (4) of three-dimensional culture and myofibroblasts monolayer (5). GAPDH was used as loading control. Representative image of three independent experiments is shown. (B) Densitometric analysis of α-SMA protein levels. Data are reported as mean ±SE. * $p<0.05$ for 2 vs 3 and 3 vs 4; °$p<0.01$ for 1 vs 3 and 3 vs 5; #$p<0.0001$ for 1 vs 5, 2 vs 5 and 4 vs 5.

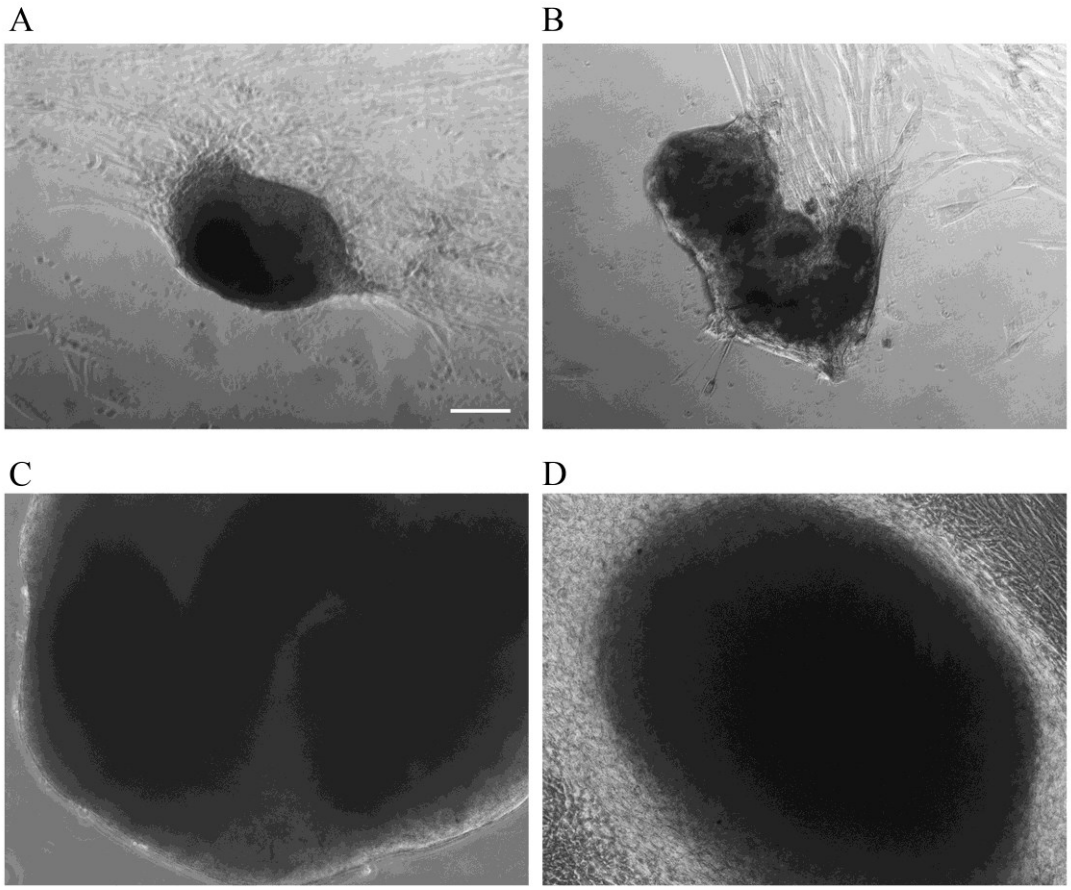

Figure 19

Clusters and spheroids formed spontaneously, without using hanging-drops and agarose-coated U-bottom well plates methods. (A, B) Clusters formed onto bottom of 12-well plastic plates. (C) Spheroid formed onto glass bottom 12-well culture plates and reverted to adhesion growth (D). Scale bar 100µm. Magnification X10.

Chapter 8

BIBLIOGRAPHY

1. Tarin D and Croft CB. *Ultrastructural features of wound healing in mouse skin.* Journal of Anatomy 1969; 105:189-190

2. Vaheri A, Enzerink A, Rasanen KP et al. *Nemosis, a novel way of fibroblast activation, in inflammation and cancer.* Experimental Cell Research 2009; 315:1633-1638

3. Sriram G, Bigliardi PL and Bigliardi-Qi M. *Fibroblast heterogeneity and its implications for engineering organotypic skin models in vitro*. European Journal of Cell Biology 2015; 94:483-512

4. Marinova-Mutafchieva L, Taylor P, Funa K et al. *Mesenchymal cells expressing bone morphogenetic protein receptors are present in the rheumatoid arthritis joint*. Arthritis and rheumatism 2000; 43(9): 2046-2055

5. Harris J. *Differentiated cells and the maintenance of tissues. In Molecular Biology of the Cell*. Alberts, B. et al., eds) 1994; 1139-1193

6. Buckley CD, Pilling D, Lord JM et al. *Fibroblasts regulate the switch from acute resolving to chronic persistent inflammation*. Trends in Immunology 2001; 22:199-204

7. Komuro T. *Re-evaluation of fibroblasts and fibroblast-like cells.* Anatomy and embryology 1990; 182:103–112

8. Lindner D, Zietsch C, Becher PM et al. *Differential expression of matrix metalloproteases in human fibroblasts with different origins*. Biochem Research International 2012; 875742

9. Brouty-Boye D, Pottin-Clemenceau C, Doucet C et al. *Chemokines and cd40 expression in human fibroblasts.* European Journal of Immunology 2000; 30:914-919

10. Chang HY, Chi JT, Dudoit S et al. *Diversity, topographic differentiation, and positional memory in human fibroblasts*. Proceedings of the National Academy of

Sciences USA 2002; 99:12877-12882

11. Van Linthout S, Miteva K and Tschöpe C. *Crosstalk between fibroblasts and inflammatory cells.* Cardiovascular Research 2014; 102:258-269

12. Parsonage G, Falciani F, Burman A et al *Global gene expression profiles in fibroblasts from synovial, skin and lymphoid tissue reveals distinct cytokine and chemokine expression patterns.* Thrombosis and Haemostasis 2003; 90:688-697

13. Kalluri R and Zeisberg M. *Fibroblasts in cancer*. Nature Reviews Cancer 2006; 6:392-401

14. Arcucci A, Ruocco MR, Granato G et al. *Cancer: an oxidative crosstalk between solid tumor cells and cancer associated fibroblasts.* Biomed Research International 2016; 2016:4502846

15. Parsonage G, Filer AD, Haworth O et al. *A stromal address code defined by fibroblasts*. Trends of Immunology 2005; 26:150-156

16. Salmenperä P, Karhemo PR, Räsänen K et al. *Fibroblast spheroids as a model to study sustained fibroblast quiescence and their crosstalk with tumor cells.* Experimental Cell Research 2016; 345:17-24

17. Tomasek JJ, Gabbiani G, Hinz B et al. *Myofibroblasts and mechano-regulation of connective tissue remodelling.* Nature reviews molecular cell biology 2002; 3(5):349-363

18. Hinz B, Mastrangelo D, Iselin CE, et al. *Mechanical Tension Controls Granulation Tissue Contractile Activity and Myofibroblast Differentiation.* The American Journal of pathology 2001; 159(3):1009-1020

19. Hinz B, Celetta G, Tomasek JJ, et al. *Alphasmooth muscle actin expression upregulates fibroblast contractile activity.* Molecular Biology of the Cell 2001; 12:2730-2741

20. Ffrench-Constant C, Van De Water L, Dvorak HE et al. *Reappearance of an Embryonic Pattern of Fibronectin Splicing during Wound Healing in the Adult Rat*. Journal Cell Biology 1989; 109(2): 903-914

21. Dugina V, Fontao L, Chaponnir C, et al. *Focal adhesion features during myofibroblastic differentiation are controlled by intracellular and extracellular factors.* Journal of Cell Science 2001; 114:3285-3396

22. Darby I, Skalli O and Gabbiani G. *Alpha-smooth muscle actin is transiently expressed by myofibroblasts during experimental wound healing*. Laboratory Investigation 1990; 63:21-29

23. Serini G and Gabbiani G. *Mechanisms of myofibroblast activity and phenotypic modulation.* Experimental Cell Research 1999; 250:273-283

24. Burridge K and Chrzanowska-Wodnicka M. *Focal adhesion, contractility and signalling.* Annual Review of Cell and Developmental Biology 1996; 12:463-518

25. Ehrlich HP and Diez T. *Role for gap junctional intercellular communications in wound repair.* Wound Repair and Regeneration 2003; 11:481-489

26. Spanakis SG, Petridou S and Masur SK. *Functional gap junctions in corneal fibroblasts and myofibroblasts.* Investigative ophthalmology & visual science 1998; 39:1320-1328

27. Clayton A, Evans RA, Pettit E et al. *Cellular activation through the ligation of intercellular adhesion molecule-1.* Journal of Cell Science 1998; 111:443-453

28. Zeisberg M., Strutz F and Muller GA. *Role of fibroblast activation in inducing interstitial fibrosis.* American Journal of Nephrology 2000; 13:S111-S120

29. Vaughan MB, Howard EW and Tomasek JJ. *Transforming growth factor-β1 promotes the morphological and functional differentiation of the myofibroblast*. Experimental Cell Research 2000; 257:180-189

30. Ronnov-Jessen L and Petersen OW. *Induction of α-smooth muscle actin by transforming growth factor-β1 in quiescent human breast gland fibroblasts. Implications for myofibroblast generation in breast neoplasia.* Laboratory Investigation 1993; 68:696–707

31. Borsi L, Castellani P, Risso AM et al. *Transforming growth factor-β regulates the splicing pattern of fibronectin messenger RNA precursor*. FEBS Letters 1990; 261(1):175-178

32. Jain RK, Martin JD and Stylianopoulos T. *The role of mechanical forces in tumor growth and therapy.* Annual Review of biomedical engineering. 2014; 16:321-346

33. Liu M, Xu J and Deng H. *Tangled fibroblasts in tumor stroma interactions*. International Journal of Cancer 2011; 129:1795-1805

34. Zhang Y, Cao HJ, Graf B et al. *CD40 engagement up-regulates cyclooxygenase-2 expression and prostaglandin E2 production in human lung fibroblasts*. Journal of Immunology 1998; 160(3):1053–1057

35. Desmouliere A, Guyot C and Gabbiani G. *The stroma reaction mypfibroblast: a key player in the control of tumor cell behavour.* International Journal of Developmental Biology 2004; 48:509-517

36. da Rocha-Azevedo B and Grinnell F. *Fibroblast morphogenesis on 3D collagen matrices: the balance between cell clustering and cell migration*. Experimental cell research 2013; 319(16):2440-2446

37. Öhlund D, Elyada and Tuveson D. *Fibroblast heterogeneity in the cancer wound.* Journal of Experimental Medicine 2014; 211:1503-1523

38. Bizik J, Kankuri E, Ristimaki A et al. *Cell-cell contacts trigger programmed necrosis and induce cyclooxygenase-2 expression.* Cell death and differentiation 2004; 11(2):183-195

39. Hynes RO. *Integrins: bidirectional allosteric signaling machines.* Cell 2002; 110: 673-687

40. Werner S and Grose R. *Regulation of wound healing by growth factors and cytokines.* Physiological Reviews 2003; 83:835–870

41. Eming SA, Krieg T and Davidson JM. *Inflammation in wound repair: molecular and cellular mechanisms.* Journal of Investigative Dermatology 2007; 127:514–525

42. Desmouliere A, Redard M, Darby I, et al. *Apoptosis mediates the decrease in cellularity during the transition between granulation tissue and scar*. The American Journal of pathology 1995; 146:56-66

43. Ehrlich HP, Desmouliere A, Diegelmann RF et al. *Morphological and immunochemical differences between kelois and hypertrophic scar*. The American Journal of pathology 1994; 145:105-113

44. Matsumoto K and Nakamura T. *Hepatocyte growth factor and the Met system as a mediator of tumor-stromal interactions*. International Journal of Cancer 2006; 119:477-483

45. Ingber DE. *Cancer as a disease of epithelial-mesenchymal interactions and extracellular matrix regulation.* Differentiation 2002; 70:547-560

46. Arnold KM, Opdenaker LM, Flynn D et al. *Wound Healing and Cancer Stem Cells: Inflammation as a Driver of Treatment Resistance in Breast Cancer.* Cancer Growth metastasis 2015; 8:1-13

47. Quaranta V. *Motility cues in the tumor microenvironment*. Differentiation 2002; 70:590-598

48. Orimo A and Weinberg RA. *Stromal fibroblast in cancer. A novel tumor-promoting cell type.* Cell Cycle 2006; 5:1597-1601

49. De Wever O, Demetter P, Mareel M et al. *Stromal myofibroblasta are drivers of invasive cancer growth*. International Journal of Cancer 2008; 123:2229-2238

50. Tlsty TD and Coussens LM. *Tumor stroma and regulation of cancer development.* Annual Review of Pathology Mechanisms of Disease 2006; 1:119–150

51. Orimo A, Gupta PB, Sgroi DC et al. *Stromal fibroblasts present in invasive human breast carcinomas promote tumor growth and angiogenesis through elevated SDF-1/CXCL12 secretion.* Cell 2005; 121:335-348

52. Ostman A and Augsten M. *Cancer-associated fibroblasts and tumor growth-bystanders turning into key players.* Current Opinion in Genetics & Development 2009; 67-73

53. Augsten M. *Cancer associated fibroblasts as another polarized cell type of the tumor microenvironment*. Frontiers in oncology 2014; 4:62

54. Hinz B, Phan SH, Thannickal VJ et al. *Recents developmentsin myofibroblasts biology: paradigms for connective tissue remodelling.* The American journal of pathology 2012; 180(4):1340-1355

55. Cirri P and Chiarugi P. *Cancer associated fibroblasts: the dark side of the coin*. American Journal of Cancer Research 2011; 1:482-497

56. Toullec A, Gerald D, Despouy G et al. *Oxidative stress promotes myofibroblast differentiation and tumour spreading* EMBO Molecular medicine 2010; 2(6): 211–230

57. Pampaloni F, Reynaud EG and Stelzer EHK. *The third dimension bridges the gap between cell culture and live tissue.* Molecular cell biology 2007; 8:839-845

58. Griffith LG and Swartz MA. *Capturing complex 3D tissue physiology in vitro.* Nature Reviews Molecular Cell Biology 2006; 7:211-224

59. Abbott A. *Cell culture: Biology's new dimension*. Nature 2003; 424:870-872

60. Hanahan D and Weinberg RA. *The hallmarks of cancer*. Cell 2000; 100:57-70

61. Kunz-Schughart LA and Knuechel R. *Tumor-associated fibroblasts (part I): Active stromal participants in tumor development and progression?* Journal of Histology & Histopathology 2002; 17:599-621

62. Eritja N, Dolcet X and Matias-Guiu X. *Three-dimensional epithelial cultures: a tool to model cancer development and progression.* Journal of Histology & Histopathology 2013; 28:1245-1256

63. Mueller-Klieser W. *Tree-dimensional cell cultures: from molecular mechanisms to clinical applications* American journal of physiology, 1997; 273: 1109-1123

64. Lin RZ and Chang HY. *Recent advances in three-dimensional multicellular spheroid culture for biomedical research.* Biothecnology Jounal 2008; 3:1172-1184

65. Kunz-Schughart LA, Kreutz M and Knuechel R. *Multicellular spheroids: a three-dimensional in vitro culture system to study tumour biology.* International Journal Of Experimental Pathology 1998; 79:1-23

66. Xia L, Sakban RB, Qu Y et al. *Tethered spheroids as an in vitro hepatocyte model for drug safety screening*. Biomaterials 2012; 33:2165-2516

67. Friedrich J, Seidel C, Ebner R, et al. *Spheroid-based drug screen: considerations and practical approach.* Nature Protocols 2009; 4:309-324

68. Dubessy C, Merlin JM, Marchal C et al. *Spheroids in radiobiology and photodynamic therapy.* Critical Reviews in Oncology/Hematology 2000; 36:179-192

69. Hirschhaeuser F,Menne H, Dittfeld C et al. *Multicellular tumor spheroids: an underestimated tool is catching up again.* Journal of Biotechnology 2010; 148:3-15

70. Burdett E, Kasper FK, Mikos AG et al. *Engineering tumors: a tissue engineering perspective in cancer biology.* Tissue Engineering Part B Reviews 2010; 16:351-359

71. Sutherland RM and Durand RE. *Radiation Response of Multlcell Spherolds: an in vitro tumour model.* Current topics in radiation research quarterly 1976; 11:87-139

72. Kunz Schughart LA and Mueller-Klieser W. *Tree-dimensional culture* In masters JRW editor Animal Cell culture A practical approach,3rd edition 2000; 123-184

73. Lawlor ER, Scheel C, Irving, J et al. *Anchorage-independent multi-cellular spheroids as an in vitro model of growth signaling in ewing tumors*. Oncogene 2002; 21:307

74. Myatt SS, Redfern CP and Burchill SA. *P38mapkdependent sensitivity of Ewing's sarcoma family of tumors to fenretinide-induced cell death*. Clinical Cancer Research 2005; 11:3136

75. Mironov V, Visconti RP, Kasynov V et al *Organ printing: tissue spheroids as building blocks.* Biomaterials 2009; 30: 2164-2174

76. Dror S, Sander L, Schwartz H et al. *Melanoma miRNA trafficking controls tumour primary niche formation.* Natural Cell Biology 2016; 18(9):1006-1017

77. Sutherland RM, McCredle JA and Inch WR. *Growth of multicell spheroids in tissue culture as a model of nodular carcinomas.* Journal of the National Cancer institute 1971; 46(1):113-120

78. Yuhas JM, Li AP, Martinez AO et al. *A simplified method for production and growth of multicellular tumor spheroids.* Cancer Research 1977; 37:3639-3643

79. Song H, David O, Clejan S et al. *Spatial composition of prostate cancer spheroids in mixed and static cultures*. Tissue Engeenering. 2004; 10:1266-1276

80. Friedrich J, Ebner R and Kunz-Schughart LA. *Experimental anti-tumor therapy in 3-D: spheroids--old hat or new challenge?* International journal of radiation biology 2007; 83(11-12):849-871

81. Carlsson J, Nilsson K,Westermark B et al. *Formation and growth of multicellular spheroids of human origin.* International Journal of Cancer 1983; 31:523-533

82. Ivascu A and Kubbies M. *Rapid Generation of Single-Tumor Spheroids for High-Throughput Cell Function and Toxicity Analysis.* Journal of Biomolecular Screening 2006; 11:922-932

83. Santini MT and Rainaldi G. *Three-dimensional spheroid model in tumor biology*. Pathobiology 1999; 67:148-157

84. Hubbell JA. *Biomaterials in tissue engineering*. Biotechnology NY 1995; 13:565

85. Timmins NE and Nielsen LK. *Generation of multicellular tumor spheroids by the hanging-drop method*. Methods in Molecular Medicine 2007; 140-141

86. Kelm JM, Timmins NE, Brown CJ et al. *Method for generation of homogeneous multicellular tumor spheroids applicable to a wide variety of cell types.* Biotechnology and Bioengineering 2003; 20:83:173-180

87. Keller GM. *In vitro differentiation of embryonic stem cells*. Current Opinion in Cell Biology 1995; 7:862-869

88. Hescheler J, Fleischmann BK, Lentini S et al. *Embryonic stem cells: a model to study structural and functional properties in cardiomyogenesis.* Cardiovascascular Research. 1997; 36(2):149-162

89. Kurosawa H. *Methods for inducing embryoid body formation: in vitro differentiation system of embryonic stem cells*. Biotechnology and Bioengineering 2007; 103:389-398

90. Huang Y, Chan C, Lin W et al. *Scalable production of controllable dermal papilla spheroids on PVA surfaces ant the effects of spheroid size on hair follicle regeneration.* Biomaterials 2013; 34:442-451

91. Chan HF, Zhang Y, Ho Y et al. *Rapid formation of multicellular spheroids in double-emulsion droplets with controllable microenvironment*. Scientific Reports 2013; 3:3462

92. Fukuda J, Khademhosseini A, Yeo Y et al. *Micromolding of photocrosslinkable chitosan hydrogel for spheroid microarray and co-cultures*. Biomaterials 2006, 27: 5259-5267

93. Karp JM, Yeh J, Eng G et al. *Controlling size, shape and homogeneity of embryoid bodies using poly (ethylene glycol) microwells.* Lab on a Chip 2007; 7:786-794

94. Zhao Z, Gu J, Zhao Y et al. *Hydrogel Thin Film with Swelling-Induced Wrinkling Patterns for High-Throughput Generation of Multicellular Spheroids* Biomacromolecules 2014; 15(9):3306-3312

95. Rickham PP. *Human experimentations. Code of ethics of the World Medical Association. Declaration of Helsinki*. British Medical Journal 1964; 18;2(5402):177

96. Frongia C, Lorenzo C, Gianni F et al. *3D imaging of the response to CDC25 inhibition in multicellular spheroids.* Cancer Biology & Therapy 2009; 23:2230-2236

97. Gavrieli Y, Sherman Y and Ben Sasson SA. *Identification of programmed cell death in situ via specific labelling of nuclear DNA fragmentation*. Journal Cell Biology 1992; 119:493-501

98. Bradford MM *A rapid and sensitive method for the quantitation of microgram quantities of protein utilizing the principle of protein–dye binding*. Analytical Biochemistry 1976; 72:248-254

99. Cory G. *Scratch-wound assay.* Methods in Molecular Biology 2011; 769:25-30

100. Mascia A, Gentile F, Izzo A, et al. *Rab7 Regulates CDH1 Endocytosis, Circular Dorsal Ruffles Genesis and Thyroglobulin Internalization in a Thyroid Cell Line*. Journal of cell Physiology 2015; 9999:1-14

101. Herrmann H, Bär H, Kreplak L et al. *Intermediate filaments: from cell architecture to nanomechanics.* Nature Reviews Molecular Cell Biology2007; 8:562-573

102. Matthijs Blankesteijn W. *Has the search for a marker of activated fibroblasts finally come to an end?* Molecular and Cellular Cardiology 2015; 88:120-123

103. Kyrylkova K, Kyryachenko S, Leid M et al. *Detection of apoptosis by TUNEL assay.* Methods in molecular biology 2012; 887:41-47

104. Räsänen K, Salmenperä P, Baumann M et al. *Nemosis of fibroblasts is inhibited by benign HaCaT keratinocytes but promoted by malignant HaCaT cells.* Molecular Oncology 2008; 2:340-348

105. Räsänen K and Vaheri A. *Proliferation and motility of HaCaT keratinocyte derivatives is enhanced by fibroblast nemosis.* Experimental Cell Research 2010; 316(10):1739-1747

106. Mosmann T. *Rapid colorimetric assay for cellular growth and survival: Application to proliferation and cytotoxicity assays*. Journal of Immunology Methods 1983; 65:55-63

107. Peura M, Bizik J, Salmenpera P et al. *Bone marrow mesenchymal stem cells undergo nemosis and induce keratinocyte wound healing utilizing the HGF/c-Met/PI3K pathway.* Wound repair regeneration 2009; 17:569-577

108. Arnoldi R, Chaponnier C, Gabbiani G et al. *Smooth muscle. heterogeneity In: Muscle: fundamental biology and mechanisms of disease.* Hill JA and Olson EN, editors 2012;1183-1195

109. Santiago JJ, Dangerfield AL, Rattan SG et al. *Cardiac Fibroblast to Myofibroblast Differentiation In Vivo and In Vitro: Expression of Focal Adhesion Components in Neonatal and Adult Rat Ventricular Myofibroblasts*. Developmental dynamics: an

official pubblication of the American association of anatomists 2010; 239(6):1573-1584

110. Iyer VR, Eisen MB, Ross DT et al. *The transcriptional program in the response of human fibroblasts to serum*. Science 1999; 283:83-87

111. Katoh K, Kano Y, Masuda M et al. *Isolation and Contraction of the Stress Fiber*. Molecular Biology of the Cell 1998; 9:1919-1938

112. Esue O, Carson AA, Tseng Y et al. *A Direct Interaction between Actin and Vimentin Filaments Mediated by the Tail Domain of Vimentin*. The Journal of Biology 2006; 281(41): 30393–30399

113. Delehedde M, Lyon M, Vidyasagar R et al. *Hepatocyte growth factor/scatter factor binds to small heparin-derived oligosaccharides and stimulates the proliferation of human HaCaT keratinocytes*. Journal Of Biological Chemistry 2002; 277:12456-12462

114. Hinitt CA, Wood J, Lee SS et al. *BAG-1 enhances cell-cell adhesion, reduces proliferation and induces chaperone-independent suppression of hepatocyte growth factor-induced epidermal keratinocyte migration*. Experimental cell research 2010; 316:2042-2060

115. Zhang YW and Vande Woude GF. *HGF/SF-met signaling in the control of branching morphogenesisand invasion*. Journal of cell biochemistry 2003;88(2):408 417

116. Zhou L, Yang K, Andl T et al. *Perspective of Targeting Cancer-Associated Fibroblasts in Melanoma.* Journal of Cancer 2015; 6:717-726

117. Furge KA, Zhang YW and Vande Woude GF. *Met receptor tyrosine kinase: Enhanced signaling through adapter proteins.* Oncogene 2000; 19:5582–5589

118. Comoglio PM. *Pathway specificity for Met signaling*. Nature Molecular Cell Biology 2001; 3:E161-E162

119. Santoro MM and Gaudino G. *Cellular and molecular facets of keratinocyte reephitalization during wound healing.* Experimental Cell Research 2005; 304:274-286

120. Guo Y, Xie J, Rubin E et al. *Frzb, a secreted Wnt antagonist, decreases growth and invasiveness of fibrosarcoma cells associated with inhibition of Met signaling.* Cancer research 2008; 68(9):3350-3360

121. Gweon EJ and Kim SJ. *Resveratrol induces MMP-9 and cell migration via the p38 kinase and PI-3K pathways in HT1080 human fibrosarcoma cells.* Oncology

Reports 2013; 29(2): 826-834

122. Scholzen T and Gerdes J. *The Ki-67 protein: from the known and the unknown*. Journal of cell Physiology 2000;182:311-322

123. Darby IA, Laverdet B, Bonté F et al. *Fibroblasts and myofibroblasts in wound healing.* Clinical, Cosmetic and Investigational Dermatology 2014; 7:301-311

124. Kisseleva T, Cong M, Paik Y et al. *Myofibroblasts revert to an inactive phenotype during regression of liver fibrosis.* Proceedings of the National Academy of Sciences 2012; 109:9448-945